POLITECNICO DI TORINO
Repository ISTITUZIONALE

Electrification of the yacht sector via fuel cell systems for hoteling applications: A comprehensive assessment of hydrogen, ammonia, and methanol as energy carriers

Original
Electrification of the yacht sector via fuel cell systems for hoteling applications: A comprehensive assessment of hydrogen, ammonia, and methanol as energy carriers / Massaro, M.C., Revello, E., Marocco, P., Santarelli, M., Gandiglio, M., Monteverde, A.. - In: ENERGY CONVERSION AND MANAGEMENT. X. - ISSN 2590-1745. - ELETTRONICO. - 30:(2026), pp. 1-18. [10.1016/j.ecmx.2026.101902]

Availability:
This version is available at: 11583/3013512 since: 2026-07-24T11:03:40Z

Publisher:
Elsevier

Published
DOI:10.1016/j.ecmx.2026.101902

Terms of use:

This article is made available under terms and conditions as specified in the corresponding bibliographic description in the repository

Publisher copyright

(Article begins on next page)

28 October 2026

Energy Conversion and Management: X 30 (2026) 101902

Contents lists available at ScienceDirect

Energy Conversion and Management: X

journal homepage: www.sciencedirect.com/journal/energy-conversion-and-management-x

Electrification of the yacht sector via fuel cell systems for hoteling applications: A comprehensive assessment of hydrogen, ammonia, and methanol as energy carriers

Maria Chiara Massaro [a], Elisa Revello [a], Paolo Marocco [b], Massimo Santarelli [b], Marta Gandiglio [b,*], Alessandro Monteverde [a]

[a] Department of Applied Science and Technology, Politecnico di Torino, Corso Duca degli Abruzzi 24, 10129 Torino, Italy
[b] Department of Energy, Politecnico di Torino, Corso Duca degli Abruzzi 24, 10129 Torino, Italy

ARTICLE INFO

Keywords:
Yacht electrification
Hydrogen storage
PEM fuel cell
Green methanol
Green ammonia
Marine energy systems

ABSTRACT

The urgent need to decarbonize the maritime sector presents one of the most pressing and complex challenges in achieving global sustainability goals, given the unique energy and operational demands of vessels. This research investigates the electrification potential for covering the hoteling demands on-board a 35–45 m yacht, using hydrogen feeding proton exchange membrane fuel cells (PEMFCs). The yachting sector is here adopted as a technologically demanding case study for integrating unconventional fuels and fuel cell systems, since hoteling represents the largest share of the total onboard energy consumption and poses stringent constraints on space and safety. Various hydrogen storage methods are explored, including physical storage with compressed hydrogen and chemical storage via liquid chemical intermediates such as methanol and ammonia, to assess the most feasible solution for onboard installation. To optimize system operation, multiple fuel cell configurations are evaluated, encompassing both low-temperature (LT-PEMFC) and high-temperature (HT-PEMFC) options, along with their potential future improvements. Additionally, a seawater-cooled, liquid-based thermal management system is employed.

Findings indicate that green methanol and green ammonia emerge as the most viable solutions for such application, each offering specific advantages in terms of weight impact, volume requirements, and power-to-power efficiency. Moreover, the adopted holistic approach promotes the strategic use of liquid chemical carriers and underscores the significance of efficient power devices when evaluating power-to-power scenarios, encompassing net power output and auxiliary energy consumption. Although focused on yachts, the findings of this study offer valuable perspectives that may provide insights for the development of alternative energy solutions in other maritime applications.

1. Introduction

Maritime transport currently contributes for about 3% of anthropogenic global greenhouse gas (GHG) emissions and involves an annual consumption of 339 Mt of heavy oil. To reach net-zero GHG emissions, the updated 2023 International Maritime Organization (IMO) introduced several strategies. In particular, a reduction in carbon intensity of international shipping by at least 40% compared to the reference year 2008 has been established by 2030, encouraging near-zero emission technologies and fuels [1].

An initial measure implemented by the IMO was the Energy Efficiency Design Index (EEDI), enforced since 2013. The EEDI promotes the utilization of energy-efficient equipment and engines in the design of new vessels, thereby serving as a driving force for ongoing innovation and technical advancement throughout the ship design process. In 2021, the IMO fortified its initiatives by introducing two additional measures: the Energy Efficiency Existing Ship Index (EEXI) and the Carbon Intensity Indicator (CII), effective from 2023. The EEXI framework empowers shipowners and charterers to select the most fitting methods for complying with IMO regulations. Available technologies include engine/shaft power limitation, waste heat recovery, and wind-assisted propulsion. The CII rating is assigned to each ship and reflects its operational energy efficiency; the carbon intensity can be improved with

* Corresponding author.
E-mail address: marta.gandiglio@polito.it (M. Gandiglio).

https://doi.org/10.1016/j.ecmx.2026.101902
Received 8 May 2025; Received in revised form 17 April 2026; Accepted 26 April 2026
Available online 28 April 2026
2590-1745/© 2026 The Authors. Published by Elsevier Ltd. This is an open access article under the CC BY-NC license (http://creativecommons.org/licenses/by-nc/4.0/).

Nomenclature

Acronyms

BoP	Balance of Plant
CII	Carbon Intensity Indicator
CTP	Chemical-to-power
DMFC	Direct-methanol fuel cell
DOE	US Department of Energy
EEDI	Energy Efficiency Design Index
EEXI	Energy Efficiency Existing Ship Index
FC	Fuel cell
GHG	Greenhouse gas
HFO	Heavy fuel oil
HT-PEMFC	High-temperature proton exchange membrane fuel cell
IMO	International Maritime Organization
LHV	Lower heating value
LT-PEMFC	Low-temperature proton exchange membrane fuel cell
MCFC	Molten carbonate fuel cell
MEA	Membrane electrode assembly
MGO	Marine gas oil
MR	Membrane reactor
PAFC	Phosphoric acid fuel cell
PBR	Packed-bed reactor
PEMFC	Proton exchange membrane fuel cell
PTP	Power-to-power
SOFC	Solid oxide fuel cell
TMS	Thermal management system
WTT	Well-to-tank

Symbols

c_p	Specific heat capacity, kJ kg^{-1} K^{-1}
D_{int}	Tank internal diameter, m
e_{grav}	Gravimetric energy density, kWh kg^{-1}
e_{vol}	Volumetric energy density, kWh L^{-1}
k_s	Stress equilibrium factor
L	Total tank length, m
l	Internal length of the cylinder body, m
$\dot{m}_{carrier}$	Total flow rate of the energy carrier, kg s^{-1}
$m_{coolant}$	Mass of fuel cell coolant, kg
$\dot{m}_{coolant}$	Coolant mass flow rate, kg s^{-1}
$\dot{m}_{H_2,dayanchor}$	Hydrogen mass flow rate during day anchor operation, kg s^{-1}
$m_{H_2,required}$	Total mass of required hydrogen based on yacht autonomy, kg
$m_{H_2,tank}$	Mass of hydrogen stored in a tank, kg
m_i	Mass of component i, kg
m_{system}	Mass of overall storage system, kg
n_{tanks}	Number of tanks
P	Pressure, MPa
p_b	Burst pressure, MPa
P_{net}	Net electrical power output, kW
P_{stack}	Electrical power produced by the fuel cell stack, kW
Q	Heat produced by fuel cell, kW
$r_{in,i}$	Tank inner radius referred to the layer i, m
r_{int}	Tank inner radius, m
R_m	Tensile strength, MPa
r_{out}	Tank outer radius, m
$R_{p,0.2}$	Yield strength, MPa
V	Operating voltage of fuel cell, V
v	Volumetric surface density for thermal management system, m^2 m^{-3}
V_i	Volume occupied by the layer i constituting the tank, m^3
$V_{ext\ rack}$	External volume of hydrogen storage rack, m^3
$V_{ext,tank}$	Tank external volume, m^3
$V_{int,tank}$	Tank internal volume, m^3
V_t	Thermodynamic theoretical voltage of fuel cell, V
$V_{total\ tanks}$	Total volume of the number of tanks, m^3
t	thickness, mm
$T_{ambient}$	Temperature of external environment, °C
$t_{circ,coolant}$	Circulation time of coolant in the closed cooling circuit, s
$T_{in,air}$	Inlet temperature of air in the closed cooling circuit
$T_{in,seawater}$	Inlet temperature of seawater in the closed cooling circuit
$T_{out,air}$	Outlet temperature of air in the closed cooling circuit
$T_{out,seawater}$	Outlet temperature of seawater in the closed cooling circuit
T_{stack}	Operating temperature of fuel cell, °C
UF	Utilization factor of hydrogen storage rack
$U_{liq-gas}$	Liquid-gas heat transfer coefficient, W m^{-2} K^{-1}
$U_{liq-liq}$	Liquid-liquid heat transfer coefficient, W m^{-2} K^{-1}
w	Gravimetric surface density for thermal management system, kg m^{-2}
ρ_i	Density of i, kg m^{-3}
σ_f	Fiber strength, MPa
η_{CTP}	Chemical-to-power efficiency
$\eta_{FC,dayanchor}$	Fuel cell efficiency during day anchor operation
η_{PTP}	Power-to-power efficiency
η_{WTT}	Well-to-tank efficiency
ΔH_r	Molar enthalpy of reaction, kJ mol^{-1}
ΔT	Difference of temperature, °C

different strategies, including speed optimization, biofouling management and the employment of alternative fuels [2].

1.1. Decarbonization of the yachting sector

Luxury boats represent a small sub-sector of the maritime industry, but they offer fertile ground for cutting-edge technological developments thanks to their ample investment potential and constrained vessel dimensions. By capitalizing on opportunities within the yachting sector, technologies can be developed and optimized on a smaller scale before being scaled up, positioning the sector as a leader in driving sustainability and efficiency within the maritime domain.

The environmental impact of luxury yachts remains relatively low due to their seasonal utilization, low power requirements, and minimal representation within the global maritime fleet. However, emissions from these vessels contribute to broader issues such as air quality reduction, public health impacts, and greenhouse gas emissions, particularly in coastal areas [3]. Consequently, the emphasis on sustainability is primarily motivated by the necessity to uphold a positive image and meet customer expectations and port regulations.

In response to this awareness, several companies in the sector are investing in innovation to integrate more sustainable technologies into their products. For instance, German superyacht manufacturer Lürssen claims to have a superyacht equipped with a proton exchange membrane fuel cell (PEMFC) under construction, set for delivery in 2025. Similarly, France's Energy Observer Developments (EODev) has developed a 22 kW PEMFC system certified by Bureau Veritas, installed on the "Energy Observer", a 30-meter-long yacht, which circumnavigates the globe using hydrogen produced from renewable sources like solar and wind energy. Another example is the conceptual design of the "Aqua" super-premium yacht, a 112.3-meter-long yacht designed by Dutch design company Sinot Yacht Architecture and Design, which intends to feature a 4 MW PEMFC system. In 2021, Yanmar Engine Corporation Limited successfully converted a 12.5-meter-long yacht named "EX38A"

with a 250 kW PEMFC system customized by MIRAI, and its successful practical application is expected in 2025 [4].

The Italian shipyard Sanlorenzo announced for 2024 its 50-meter superyacht featuring a methanol fuel cell system customized by Siemens. This innovation significantly reduces the vessel's ecological footprint while at anchor by powering the on-board hotel services, with plans to increase the power output of fuel cells for partial engine power by 2026 and a fully fuel-cell-powered, net-zero model by 2027 [5].

The abovementioned strategies adopted by various companies demonstrate that the use of renewable fuels combined with alternative energy systems stands out for being the leading road in the yachting sector.

Building on this foundation, a growing body of literature has emerged to explore sustainable practices and technological innovations in the luxury yachting industry, aiming to address both environmental challenges and evolving stakeholder demands.

Engelhardt et al. [6] investigated the feasibility of an integrated fuel cell system for mobile auxiliary power unit (APU), potentially for use in caravans and yachts. The system consisted of a diesel steam reforming fuel processor, a gas clean-up module, and an 80-cell PEMFC stack. The experimental study was conducted within a fuel input range of 2 kW_{th} to 6 kW_{th} and utilized two different precious-metal-based reformer catalysts. The study highlighted the sensitivity of fuel cell performance to hydrocarbon concentrations in the reformate gas and demonstrated a stable power output of 1.5 kW_{el} at a reformer input of 4 kW_{th}.

Malla [7] presented a step-by-step approach for the design and sizing of battery systems for "zero-emission" all-electric vessels. It also presents a cost comparison between all-electric vessels and traditional diesel-powered vessels. The study highlights recent advancements in lithium-ion battery technology, particularly improvements in safety, design life, and battery management systems. It suggests that lithium-ion batteries are becoming increasingly cost-competitive with diesel generators, offering high energy density and low costs, which could drive the growth of all-electric vessels over the next decade.

Bucci et al. [8] investigated different auxiliary propulsion system configurations for luxury sailing yachts, focusing on fuel consumption and operational efficiency. The study compared four configurations using a daily operational profile, with a particular emphasis on a hybrid-electric solution paired with an onboard energy storage system. The authors highlighted that the hybrid-electric system, while heavier, offered the best fuel efficiency, together with operational advantages, such as reduced noise and pollutant emissions. Additionally, the paper examined the cost dynamics, noting that while the initial capital cost (CAPEX) of the hybrid system was higher, it became competitive over time due to lower operating costs (OPEX) and the possibility of zero-emission navigation.

Coppola et al. [9] presented a concept design and feasibility study of a hybrid propulsion system for a 80 m yacht, utilizing a conventional diesel electric configuration integrated with battery and hydrogen-powered fuel cells. The hydrogen was stored as methanol and converted onboard via reforming. The study compared a conventional diesel propulsion system with the designed hybrid system, analysing various operational profiles, including stationing and sailing times. The results indicated that the amount of methanol required for the yacht's autonomy could $<$ be feasibly installed. The integration of the hybrid propulsion system, including fuel cells, reforming systems, electric motors, and frequency converters, had minimal impact on the yacht's speed, stability, hull structure, displacement, and crew capacity, making it a viable alternative to conventional systems.

Micoli et al. [10] performed a retrofitting of a mega-yacht's electric power system to achieve zero-emission status using ammonia as a hydrogen carrier and PEMFC. The study found that hydrogen production from ammonia required a bulky fuel processing system, limiting ammonia storage to 48 m3, which affected the yacht's autonomy. In Cruise Mode, autonomy was 6 days, while Full Electric Mode reduced it to 3 days. Increasing storage space could improve autonomy but would require significant modifications.

Di Bernardo et al. [11] presented the preliminary design of a 75-meter hybrid diesel-electric mega yacht. The hybrid system was equipped with four hydrogen-powered fuel cells (540 kW), two 180 kW electric motors and two 1765 kW thermal engines. The hydrogen was stored in 105 cylinders with a total capacity of 21.3 m^3 at 350 bar. The system allowed for green cruising up to 240 km or 24 h of hotel services, enabling access to marine protected areas and reducing noise.

Chen et al. [12] designed a proof-of-concept for a hydrogen-powered luxury yacht, Hydronautic+, and its supporting infrastructure, fHuel+, centred on a localized hydrogen economy. The concept proposed hydrogen production at marinas using off-peak electricity to power a PEM electrolyser, with storage and compression at the dockside. On-board, 9.70 kg of hydrogen stored at 700 bar were converted by two 114 kW PEMFCs to power an electric motor. The approach integrated conceptual design, economic analysis, life-cycle assessment (LCA), and safety evaluations through failure mode and effects analysis (FMEA), demonstrating the potential of hydrogen-powered luxury boating as an environmentally friendly alternative.

1.2. Aim and novelty of the study

While there is a growing number of initiatives by companies in the yachting sector and a broad body of literature on the use of alternative fuels within the maritime industry [13], research specifically addressing alternative fuels in the yachting sector remains relatively limited. Several studies have examined the integration of hydrogen with fuel cells to partially or fully electrify propulsion systems or power onboard systems. However, to the best of our knowledge, no comprehensive analysis has been conducted to compare the various hydrogen carriers suitable for storage onboard luxury boats in terms of weight, volume, and power-to-power efficiency when coupled with fuel cell technology.

The primary objective of this study is to investigate the technical feasibility of installing a fuel cell-based powertrain to supply electrical loads onboard small-sized yachts. The yacht configuration was selected as a particularly challenging testbed for integrating unconventional fuels – hydrogen, green methanol and ammonia – since the hoteling demand represents the largest share of the onboard energy use and the available installation space is highly constrained. Demonstrating the feasibility of such systems in this context provides insights into the integration of such systems under highly constrained conditions, although dedicated assessments are required for other vessel categories.

The study focuses on considering de-fossilized fuels stored on-board, including hydrogen, synthetic methanol and ammonia. The investigation encompasses a comprehensive analysis of various aspects, including storage solutions, components for fuel release and conversion, different fuel cell configurations for optimizing system operation and efficiency, and the potential utilization of seawater for cooling purposes.

Moreover, diverse components constituting the Balance of Plant (BoP) of the system are examined, aiming to provide a holistic understanding of the proposed alternative energy system. By addressing these aspects, this study aims to provide valuable insights into the field of maritime energy systems, paving the way for more sustainable and efficient transportation solutions in the maritime industry.

In this paper, Section 2 provides an overview of the viable options for decarbonizing the yachting sector, discussing various technologies and strategies to reduce emissions. Section 3 delves into the methodology used to size the energy storage and propulsion systems. It starts by sizing different storage methods integrated with a commercial PEMFC featuring a seawater-cooled, liquid-based thermal management system, and then optimizes the most promising storage solution with improved PEMFC technologies. Section 4 presents the results of these analyses, highlighting the performance and feasibility of the proposed solutions in terms of weight, volume, and power-to-power efficiency. Finally, Section 5 summarizes the key findings and their potential implications for advancing sustainable yachting.

2. Options for the de-fossilization of the yachting sector

Hydrogen-powered fuel cells emerge as one of the most suitable and high-efficient technologies for the de-fossilization of maritime field [14]. However, hydrogen storage and onboard integration are quite difficult due to the low volumetric energy density of hydrogen. To this purpose, Table 1 compares different storage solutions such as compressed hydrogen, liquid hydrogen, synthetic methanol and ammonia with conventional diesel, considering their gravimetric (e_{grav}) and volumetric (e_{vol}) energy densities [15].

Compressed hydrogen is the simplest and most consolidated storage method. It comprises a tank and its BoP, which includes primary pressure regulator, solenoid control valves, a fill tube or port and a pressure gauge/transducer [16]. Tank design for gaseous hydrogen must address issues like permeation and embrittlement to which the selected material is exposed. In addition, the chosen material must be lightweight and have high strength to withstand pressures ranging from 200 to 700 bar. The performance evaluation of such technology considers factors like gravimetric weight, which varies between 1 and 6 wt% depending on the vessel type and shape, and gravimetric/volumetric energy density [17,18]. Compressed hydrogen storage method enables rapid refueling and fast release of hydrogen, accommodating load changes without necessitating a buffer tank. Furthermore, it boasts a relatively high gravimetric energy density, and it is a well-established, reliable technology. However, there are notable drawbacks to consider. The compressed hydrogen storage suffers from low volumetric energy density, requiring considerable space for installation. High working pressure poses explosion risks, demanding stringent safety measures. Furthermore, the need for a rack to accommodate multiple tanks increases system weight and volume, posing logistical challenges and potentially impacting performance and efficiency.

Although liquid hydrogen presents a promising solution for increasing hydrogen density to up to 71 kg/m^3, its storage challenges have led to its exclusion from our study. These challenges are not compatible with the specific characteristics of the maritime application under consideration. Boil-off, resulting in approximately 1% hydrogen loss daily, poses significant difficulties for long-term storage, particularly for luxury boats with seasonal use. Moreover, the safety risks associated with handling cryogenic temperatures cannot be managed onboard due to a lack of specialized crew trained in such hazards.

Synthetic liquid fuels generated from hydrogen, such as methanol, ammonia and formic acid, can be used as hydrogen carrier compounds for the liquid chemical storage of hydrogen, thanks to their chemical bonds with the H atom. They can be easily transported over long distances, stored for a long time, and later decomposed to release hydrogen when needed (or to be directly converted to power in some types of technological devices).

Methanol (CH_3OH) is the simplest alcohol with the highest H/C ratio, and it has a theoretical gravimetric capacity of 12.5 wt%. At atmospheric pressure, it remains in liquid form between 176 and 338 K, offering a cost-effective storage option compared to LNG, H_2 and NH_3 [19]. Approved by the IMO as an alternative marine fuel since November 2020, methanol is versatile, serving in both conventional ship engines and fuel cells [3]. In 2-stroke diesel engines, methanol can significantly reduce CO_2 emissions by 5–10% and up to 80% when using green methanol. Additionally, it leads to substantial reductions in SO_x and NO_x emissions due to methanol's favorable physical properties, including lower combustion temperature, lower lean flammability limit, higher heat of evaporation, and a high-octane number [20]. In conjunction with fuel cells, methanol can be used directly as fuel in high-temperature fuel cells and direct-methanol fuel cells (DMFCs), or it can be reformed at moderate temperatures, either in a separate system or integrated in the fuel cell system. The reforming of methanol is an endothermic reaction which takes place through the reaction:

$$CH_3OH + H_2O \rightarrow CO_2 + 3H_2 \quad \Delta H_r = 49.2 kJmol^{-1}$$

Fuel purity requirements vary based on fuel cell type: low temperature fuel cells need high-purity hydrogen to prevent poisoning of platinum-based catalysts, while high temperature fuel cells accept lower-quality fuels. Methanol processing equipment thus depends on the implemented fuel cell type, and this significantly affects system characteristics such as efficiency, size, weight, cost, and transient behavior. Common processing steps include reforming, CO clean-up, purification, and equipment such as evaporators, burners, and desulfurization [21]. Despite its advantages, methanol presents challenges in handling and storage. Its low-flashpoint fuel demands stringent safety measures. In addition, due to its density and lower heating value, it necessitates larger tanks compared to Heavy Fuel Oil (HFO) of about 2.5 times. Methanol is toxic and corrosive toward certain materials, necessitating storage in well-ventilated areas and the use of compatible materials [22].

Ammonia (NH_3) is considered a promising hydrogen carrier because it is a no-carbon fuel with a high hydrogen content by weight (17.65 wt %), it can be liquefied under mild conditions (the vapor pressure of ammonia at room temperature is 9.2 bar) and stored on-board in a simple, inexpensive pressure vessel [23]. As for methanol, the release of hydrogen requires a dedicated equipment for the endothermic reaction of cracking:

$$2NH_3 \rightarrow N_2 + 3H_2 \quad \Delta H_r = 46.2 kJmol^{-1}$$

In addition, a series of equipment are needed, depending on the requirements of the downstream conversion technology [24]. The drawbacks related to ammonia include its toxicity for both humans and marine environment and its corrosiveness towards some materials [25].

The most efficient method for extracting energy from hydrogen, ammonia or methanol is using a fuel cell, which uses the energy stored in chemical bonds to directly generate electricity [14]. Additionally, noise and vibrations associated with fuel cells are minimal, and they are expected to require less maintenance compared to conventional combustion engines and turbines. However, one of the challenges faced with fuel cells is their limited lifetime [19]. A variety of fuel cell types with distinct characteristics has been developed: low and high temperature polymer electrolyte membrane fuel cell (LT/HT-PEMFC), phosphoric acid fuel cell (PAFC), molten carbonate fuel cell (MCFC) and solid oxide fuel cell (SOFC) [21]. Among them, the LT-PEMFC was selected as the most suitable technology due to its light weight and compactness, high efficiency, long lifetime, and zero emissions. In addition, since PEMFCs are characterized by fast start-up and load following, they can satisfy the ship power requirements needed for the different trip phases [24]. Nevertheless, LT-PEMFCs operate below 100°C, posing challenges in heat management. Hence, HT-PEMFCs are gaining traction in the maritime sector, operating up to 200°C. Despite lower efficiency, HT-PEMFCs can better manage heat due to increased driving force (temperature gradient with biosphere) and can operate in integrated conversion systems with ammonia and methanol without purification systems, thanks to their higher tolerance to fuel impurities [21]. In this context, Advent Technologies announced in 2023 a collaboration with a global energy technology company to develop sustainable marine fuel cell solutions for superyachts. Initially, the focus is on creating a 50 kW–500 kW hybrid power source using Advent's methanol-powered

Table 1
Gravimetric and volumetric energy densities of different energy storage options compared to diesel (values are reported as mean, with minimum-maximum range in parentheses) [15].

Energy carrier option	e_{grav}(kWh kg^{-1})	e_{vol}(kWh L^{-1})
Compressed hydrogen	1.40 (0.96 – 1.80)	0.60 (0.40 – 0.80)
Liquid hydrogen	2.50 (2.00–3.82)	1.32 (1.20 – 1.39)
Methanol	4.03 (3.90–4.36)	3.83 (3.64 – 3.92)
Ammonia	3.60 (3.22–3.60)	2.70 (2.56–2.78)
Diesel	8.30 (8.30–8.30)	8.15 (8.13–8.18)

Serene fuel cell systems, based on HT-PEMFC [26].

3. Methodology

Following the introduction of the selected case study for implementing the electrified system, this section outlines the sizing methodology. An initial assessment evaluates the technical feasibility of different storage technologies, including compressed hydrogen, ammonia, and methanol. During this phase, the fuel cell system is sized primarily to provide efficiency data for determining the required hydrogen quantity, with a commercial fuel cell serving as a reference. Moreover, thermal integration among components is explored to optimize overall system performance. In the final stage, the analysis deepens into a detailed evaluation of the most effective storage technology and its integration with various fuel cell technologies.

3.1. Case study description

The technical feasibility analysis focuses on the hoteling electrical demand of a 35–45 m yacht, currently powered by two diesel generators. Fig. 1 illustrates the typical load profile for hoteling requirements, based on 1000 h of operation per year. The proposed system adopts a hybrid configuration, where the electrified system primarily addresses the energy requirements during anchorage (day and night anchor), while the main engine covers the remaining demands. This electrification strategy has been chosen because, despite the relatively low power demand during anchorage, it accounts for the largest portion of the yacht's total energy consumption, offering a significant opportunity to minimize overall onboard emissions.

The design process starts from the net electrical energy required for hoteling. The gross power from the fuel cell is then determined iteratively by including auxiliary loads and operating conditions, and the stack size is selected to satisfy this net demand under the chosen operating point.

A typical daily operating profile is employed considering the following operating modes: day anchor (38%), night anchor (22%), maneuvering (7%), day cruise (15%). In this configuration, the complete hoteling energy system, with a maximum power demand slightly exceeding 100 kW, includes:

- A diesel generator and electric engine, as in the conventional system, to supply the peak power during maneuvering (100% of maximum power demand) and day cruising (53% of maximum power demand).
- A fuel cell system to ensure power during anchorage, covering 43% of the maximum hotelling demand during day anchor and 33% during night anchor. In this way, the fuel cell system can cover 2/3 of the daily anchor demand and the full night anchor demand.
- A battery storage system to supply the remaining day anchor demand which is not covered by the fuel cell system (about 21% of peak power demand). This system helps avoid oversizing the hydrogen storage.

For the hydrogen storage system, a one-week autonomy period is used as a baseline to define the design methodology. The hydrogen stored must support the fuel cell-powered hoteling operations, corresponding to a total energy requirement of 4522 kWh over a week.

The available space for the installation of the electrified system is within the yacht's hull structure, offering a total volume of 4.2 m^3. Additionally, an extra 14.7 m^3 of space above these areas could also be utilized. During installation, it is important to account for compartment shapes and safety regulations to ensure proper integration of the storage systems.

3.2. System design: Analysis of storage solutions for a commercial fuel cell system

After defining the characteristics of the case study, this paragraph provides a detailed description of the system sizing. This section serves to compare the sizes of different storage systems, while the sizing of the fuel cell is only briefly mentioned for determining the amount of required hydrogen, since it would be the same for all storage methods. The scheme of the process is represented in Fig. 2.

Once the power demand was determined, the fuel cell system can be sized. Commercial models of PEMFC stacks manufactured by PowerCell [27] were selected as the conversion unit due to their suitability and reliability. In particular, the commercial model, referred to as baseline

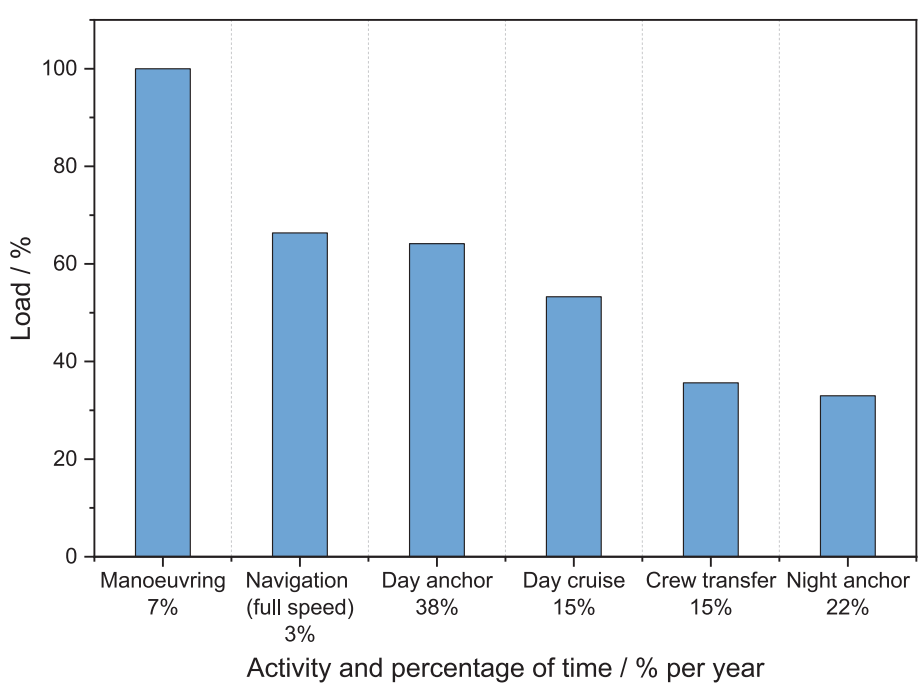

Fig. 1. 35–45 m yacht load distribution for hoteling purpose normalized to the maximum power demand, and operation time distribution over a year. Bars represent normalized power demand, while percentages below each bar indicate the fraction of operating time.

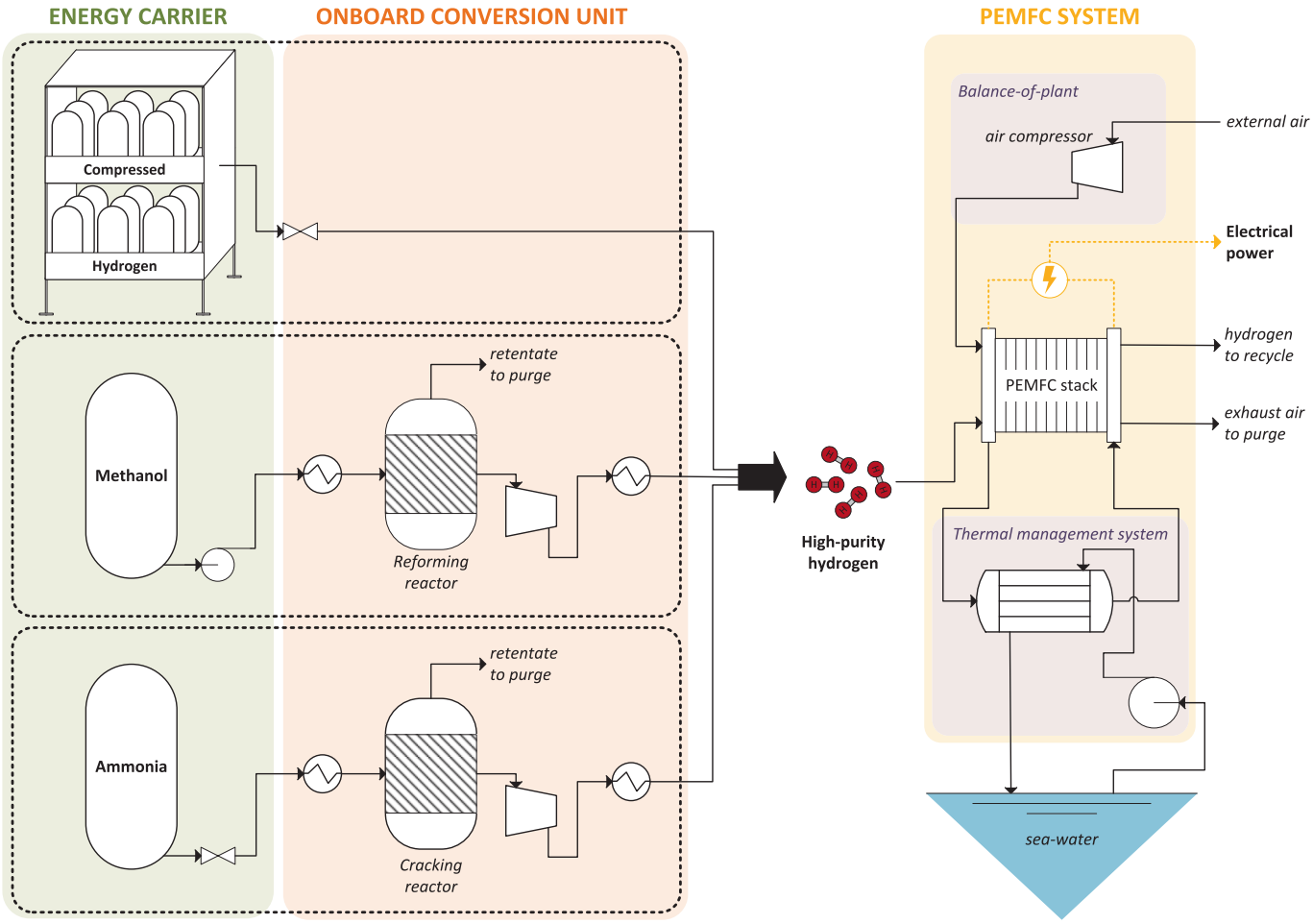

Fig. 2. Process scheme of the electrified system, accounting for three different storage methods, including compressed hydrogen, methanol and ammonia, the conversion units to release pure hydrogen, and the PEMFC system, with seawater cooled liquid-based thermal management system.

LT-PEMFC, was first defined based on the comparison of energy demands during daytime and night-time anchorage, ensuring sufficient capacity to meet peak loads. Then, considering the efficiency of the chosen PEMFC and the autonomy, the electrical consumption for the BoP (compressor, pumps, valve, etc.) and storage system were defined. Finally, the gross power requirement was calculated as the sum of the load demand and the BoP requirement and compared with the capacity of the previously selected commercial stack. If the stack's nominal power was found insufficient to meet the gross power demand, a different stack with a suitable power rating was selected from the same manufacturer, and the procedure was repeated until a convergence between the gross power demand and the size of the PEMFC was reached. A logical diagram illustrating this section is presented in Fig. 3. Various storage methods were evaluated, including gaseous hydrogen, ammonia, and methanol, while options such as methane, liquid hydrogen, and cryogenic hydrogen were excluded due to technical constraints.

3.2.1. Hydrogen storage

For the compressed hydrogen storage, two different sizing were performed, considering pressures of 350 bar and 700 bar. The procedure was the same in both cases. First, the single tank was designed to assess the weight and volume of the compressed hydrogen storage system. The amount stored in a single tank, set to 5 kg, was based on the US Department of Energy methodology [28]. Regarding the BoP, it was assumed that its components and related weight were similar for both storage pressure configurations [16]. The tank design involved two stages: a geometric design to determine the tank shape and a mechanical design to handle the working pressure.

For the geometric design, the internal volume $V_{int,tank}$ (m^3) was calculated as:

$$V_{int,tank} = \frac{m_{H_2,tank}}{\rho_{H_2}} \tag{1}$$

where $m_{H_2,tank}$ (kg) is the mass of hydrogen and ρ_{H_2} (kg m^{-3}) is the hydrogen density at the storage conditions. Hemispherical caps were chosen to simplify the evaluation of the system's weight and volume. The following formulas were used to determine the cylindrical body's length and diameter [28]:

$$V_{int,tank} = \pi \cdot r_{in}^2 \cdot l + \frac{4}{3} \cdot \pi \cdot r_{in}^3 \tag{2}$$

$$L/D_{int} = 3 \tag{3}$$

where r_{in} (m) is the internal radius of the tank, l (m) is the internal length of the cylinder body, $L = l + 2r_{in}$ (m) is the total length of the tank, D_{int} (m) is the internal diameter of the tank.

Once the tank's inner dimensions were defined, the mechanical design evaluated the stresses and consequently the thickness of the different layers. The layers involved are:

- A liner layer to prevent hydrogen permeation, made of a high-density polymer, with no structural function. This layer has a thickness $t_{liner} = 5mm$.

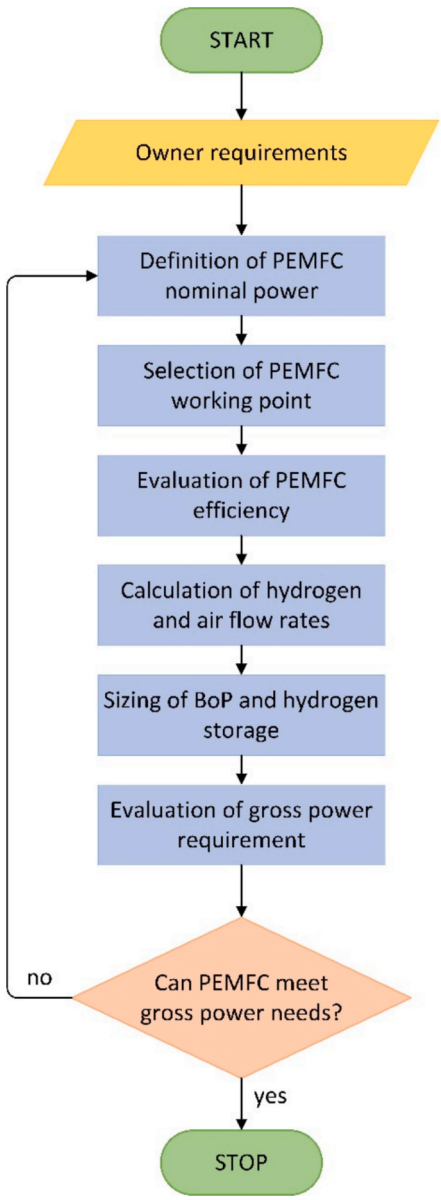

Fig. 3. Flow diagram of calculation procedure for PEMFC sizing.

- A composite layer, which forms the tank walls and handles structural functions. Its thickness was calculated to withstand working pressure stresses.
- A glass fiber layer protects the composite walls from shocks, and it has a thickness $t_{glass} = 1mm$.
- A foam layer for the dome protection, with a thickness $t_{foam} = 10mm$.

The netting theory was used to design the composite thickness $t_{composite}$ (mm), applying the following equation [29]:

$$t_{composite} = \frac{(2 \cdot k_s + 1) \cdot r_{in,composite} \cdot p_b}{2 \cdot k_s \cdot \sigma_f} \tag{4}$$

where k_s is the stress equilibrium factor, $r_{in,composite}$ (mm) is the inner radius of the composite layer, p_b (MPa) is the burst pressure, σ_f (MPa) is the fiber strength. The composite material used was Toray T700S, with a fiber content of 60% and a reduced tensile strength of 2295 MPa to account for fiber variability [28]. The stress equilibrium factor was set at 0.75 [29]. A burst pressure of 90 MPa was initially chosen for both 350 and 700 bar tanks. The stress ratio, which must be limited to 0.55 for 350 bar tanks and 0.5 for 700 bar tanks [28], was used to evaluate if the burst pressure was sufficient.

After designing the tanks operating at 350 bar and 700 bar, the weight and volume of the entire system were evaluated. This involved multiplying the weight and volume of a single tank by the number of tanks needed to achieve the required autonomy. The same procedure applies to both tank types, so the formulas are presented once. To determine the number of tanks (n_{tanks}), the following formula was used:

$$n_{tanks} = \frac{m_{H_{2,required}}}{m_{H_{2,tank}}} \tag{5}$$

where $m_{H_{2,required}}$ (kg) is the total mass of required hydrogen and $m_{H_{2,tank}}$ (kg) is the mass of hydrogen stored in a single tank.

Knowing the number of tanks, the entire system's characteristics were derived with the following formulas.

To calculate the system volume, the volume of the single tank was first determined as follows:

$$V_{tank} = V_{int,tank} + V_{liner} + V_{composite} + V_{glass} + V_{foam} \tag{6}$$

where the volume of the single layer i (i.e., liner, composite, glass fiber, and foam) was calculated based on its thickness t_i (mm) and the external radius of the layer $r_{out,i}$ (mm). Both the cylindrical and the semi-spherical parts of the tank were considered in the calculation:

$$V_i = \pi \cdot l \cdot \left[\left(r_{in,i} + t_i \right)^2 - r_{in,i}^2 \right] + \frac{4}{3} \cdot \pi \cdot \left[\left(r_{in,i} + t_i \right)^3 - r_{in,i}^3 \right] \tag{7}$$

The volume of the foam layer, differently from the others, was calculated considering only the semi-spherical domes, derived imposing $l = 0$.

The total volume occupied by the tanks was then calculated as:

$$V_{total\ tanks} = n_{tanks} \cdot V_{tank} \tag{8}$$

Finally, additional space was considered for the BoP, the rack, and the empty space between tanks. This was reflected by the utilization factor (UF), calculated as the ratio of the total tanks volume $V_{total\ tanks}$ (m^3) to the total volume occupied by the rack $V_{ext\ rack}$ (m^3):

$$UF = \frac{V_{total\ tanks}}{V_{ext\ rack}} \tag{9}$$

The value of UF (50%) was derived as an average value from the sizing procedure of various hydrogen bottles in the chosen vessel.

For the system mass, the system weight was determined by the sum of the different tank layers and the mass of hydrogen stored inside:

$$m_{system} = n_{tanks} \cdot \left(m_{liner} + m_{composite} + m_{glass} + m_{foam} + m_{BoP} + m_{H_{2,tank}} \right) \tag{10}$$

For the term related to the BoP mass (m_{BoP}), the value adopted by the DOE methodology [28] is considered in this study. This mass term includes safety devices, regulators, electronic controllers and sensors, all onboard conditioning equipment necessary to store the hydrogen as well as mounting hardware and delivery piping.

In the equation, the weight of the layer i was calculated starting from its volume V_i and density of material ρ_i as follows:

$$m_i = \rho_i \cdot V_i \tag{11}$$

The weight of the rack was not included in the evaluation of the system weight, as this depends on the configuration of the cylinders inside the yacht.

The input parameters for designing the compressed hydrogen storage system are detailed in Table A of the Appendix.

3.2.2. Methanol storage

Methanol, maintained as a liquid at ambient conditions (20°C and 1 bar), was stored according to the requirements dictated by the reforming reaction's stoichiometry. Moreover, an additional amount of methanol was considered to meet the thermal demands of the system through combustion in a dedicated burner. The sizing of the methanol tank

utilized gravimetric and volumetric indexes, yielding values of 4.03 kWh kg^{-1} and 3.83 kWh L^{-1}, respectively [15].

Similarly, the amount of water needed for the reforming reaction was calculated based on the reaction stoichiometry. The size of the water tank was determined using commercially available models manufactured by Plastic Mart, which are already employed in maritime applications [30].

Methanol-water mixture was heated and pumped to a temperature of 350°C and a pressure of 50 bar to facilitate the methanol reforming reaction, through which hydrogen was extracted from the energy carrier. Instead of using a traditional packed-bed reactor (PBR), a membrane reactor (MR) with hydrogen-selective ceramic-based carbon membrane was employed, allowing both catalytic methanol reforming and membrane separation to occur simultaneously within a single unit under the same reaction conditions. The reactor developed in the HyMethShip project [31] was selected as an innovative and promising non-commercial conversion technology and the final size was obtained through a linear scale-up, justified by the modular structure of the membrane reactor, which enables scaling through replication of identical units within the investigated range. To achieve the highest possible purity of H_2, the project considered operating with the reaction stream at 50 bar and obtaining hydrogen output at 10 bar, maximizing the pressure difference between the two sides. Under these operating conditions, membrane reactors are expected to provide enhanced methanol conversion and hydrogen recovery compared to conventional reactors due to improved reaction–separation coupling [32]. Therefore, methanol conversion > 90%, hydrogen recovery > 90%, and hydrogen purity > 99.9% were assumed, making the produced hydrogen suitable for both LT-PEMFC and HT-PEMFC applications. If required, an additional downstream purification stage could be implemented with negligible impact on the overall system weight and volume, as supported by literature [23].

Before entering the fuel cell stack, hydrogen was conditioned to the stack's operating temperature and pressure. This necessitates the use of a turbine (or alternatively an expansion valve) and a cooler.

3.2.3. Ammonia storage

Ammonia was stored in liquid form at 10 bar and ambient temperature, with a resulting density of 602 kg m^{-3}. An additional margin of empty volume of 14% was estimated as a safety factor, in order to accommodate any unexpected expansion or contraction. A table from Perry's Handbook on vertical cylindrical vessels was used as a reference [33], providing the volume, length, and diameter of the storage tank. For the design of the tank heads, tori spherical heads were chosen due to their structural advantages and space efficiency. The procedure for sizing these heads was detailed in Perry's Handbook [33]. Using the aforementioned references and procedures, the total volume of the storage tank was calculated. A crucial step in the tank design was the selection of material. The material had to withstand the corrosive nature of ammonia, leading to the choice of austenitic stainless steel AISI 316. The mechanical properties of this material are summarized in Table A of the Appendix, including the yield strength $R_{p,0.2}$ (MPa) and the tensile strength R_m (MPa).

The thickness $t_{NH_3\ tank}$ (m) of the tank wall was calculated using the following equation [33]:

$$t_{NH_3\ tank} = \frac{P \cdot D_{int}}{2 \cdot f - P} \tag{12}$$

where P (MPa) is the operating pressure, D_{int} (mm) is the internal diameter of the tank, and f is defined as:

$$f = min\left(\frac{R_{p,0.2}}{1.5}, \frac{R_m}{2.4}\right) \tag{13}$$

After calculating the thickness, an additional 2.5 mm was added as a precaution against corrosion.

Once the wall thickness was determined, the volume of the empty tank was calculated. The total weight of the storage system was the sum of the weight of the empty tank, which was evaluated using the density of the steel provided in Table A of the Appendix, and the weight of the ammonia to be stored.

By following these steps, the ammonia storage tank was appropriately sized to ensure safety and efficiency.

Subsequently, the ammonia was heated to 485°C and subjected to a cracking reaction at 9 bar in a membrane reactor derived from the study by Cerrillo et al. [34]. This reactor configuration, as described in the case of methanol, enabled both the conversion of ammonia and the purification of hydrogen within the same unit, with high-purity hydrogen exiting the reactor as permeate. Based on the experimental results reported in [34], complete ammonia conversion was assumed, together with hydrogen recovery higher than 90% and purity above 99.97%, making the produced hydrogen suitable for both LT-PEMFC and HT-PEMFC applications. Using the inlet ammonia flow rates and the outlet hydrogen flow rates as references, a linear scale-up was performed primarily to meet the energy requirements of the equipment.

For the weight and volume considerations, it was known that the reactor consists of an outer stainless-steel module with the membrane located on a porous ceramic tube. Without direct information from the analyzed study regarding the weights and volumes of such a reactor, gravimetric and volumetric indices referred to hydrogen flow rate derived by other types of intensified reactors used for the same purpose were utilized, equal to 8123 kg kg^{-1} s and 9.9 m^3 kg^{-1} s [35].

In both the ammonia- and methanol-based configurations, the hydrogen purity achieved by the membrane reactor is assumed to be sufficient to supply both LT- and HT-PEMFC systems. If necessary, an additional purification stage could be included with negligible impact on the overall system weight and volume, as demonstrated in previous work by Massaro et al. [23].

3.2.4. Auxiliary equipment for chemical energy carriers

The use of chemical carriers, i.e. methanol and ammonia, required the use of a series of auxiliary equipment in the conversion process, such as pumps, compressors, heat exchangers. In this section, the description of the sizing procedure for the auxiliary components is reported.

First, a heat exchanger was required to heat the stored fuel (methanol or ammonia) from the storage ambient temperature to the reaction temperature. A process simulation software was used for the sizing, operating in shortcut calculation mode and setting up a counter current heat exchange configuration, followed by using the design function for deriving the required heat exchange area. At this point, the indices from Table A of the Appendix were used for the final sizing [36].

An additional combustor was required in both case studies to meet the thermal requirements of the reforming and cracking processes. It needed to satisfy the demand for pre-heating the entering reactants and maintaining the reaction temperature due to their endothermic nature. Once the thermal power was calculated, it was possible to derive the amount of required fuel. Finally, the size of the combustor was derived from commercial models.

Lastly, the equipment necessary for the movement of the streams within the system was analyzed, including pumps, compressors and turbines. In this case as well, commercial models were considered based on the specific requirements.

3.2.5. Fuel cell thermal management system

The heat produced by the fuel cell stack $\boldsymbol{Q}$ (MW) was crucial to assess the size of the thermal management system (TMS), as it must be properly removed to prevent overheating of the system. It was calculated as follows:

$$Q = (1 - 0.1) \cdot \left(1 - \eta_{FC,dayanchor}\right) \cdot \dot{m}_{H_2,dayanchor} \cdot LHV_{H_2} \tag{14}$$

where $\eta_{FC,dayanchor}$ is the FC stack efficiency, $\dot{m}_{H_2,dayanchor}$ (kg s^{-1}) is the

hydrogen mass flow rate during day anchor operation and LHV_{H_2} is the lower heating value of hydrogen (120 MJ kg^{-1}); in addition, a 10% heat loss was considered to be removed with convection [37].

The TMS consists of two loops: a closed cycle where the coolant (Glysantin® [38]) extracts heat from the FC, and a second open loop where the refrigerant fluid passes through a secondary heat exchanger thermally coupled to an external cooling sink. In the standard approach, the external cooling sink consists of ambient air, and heat rejection is achieved through an air-cooled radiator operating under worst-case summer conditions. Alternatively, a second configuration was considered in which the air radiator is replaced by a liquid-to-liquid heat exchanger using seawater as the external cooling medium.

In this case, the seawater temperature was assumed under worst-case summer conditions, and a fouling factor was included in the sizing calculations to account for performance degradation associated with marine water operation. This approach ensures that the thermal management system is sized under design-limiting conditions, resulting in a conservative system configuration.

The assumed seawater fouling factor, equal to 0.00009 m^2 K W^{-1} contributes less than 3% to the overall thermal resistance of the heat exchanger. This contribution is significantly lower than typical design margins and uncertainties associated with heat transfer correlations. Moreover, given the seasonal operation profile of yachts, prolonged and intensive seawater exposure is limited, thereby reducing the practical impact of fouling over the operating lifetime.

The design of the heat exchanger was determined using the ε-NTU method [39]. The input parameters used in the sizing procedure are summarized in Table A of the Appendix.

Finally, the weight and volume of the heat exchanger were determined using gravimetric and volumetric surface densities, as reported in Table A of the Appendix. The required coolant mass $m_{coolant}$ (kg) was also estimated, assuming a suitable circulation time $t_{circ,coolant}$ (s):

$$m_{coolant} = \dot{m}_{coolant} \cdot t_{circ,coolant} \tag{15}$$

Remaining components such as pipes, pumps and fan are expected to contribute to an additional 20% of the total weight of the cooling system [40].

Subsequently, this methodology was used for the sizing of a seawater cooling system. In this case, the liquid–liquid heat transfer ($U_{liq-liq}$) is most favorable compared to the gas–liquid heat transfer ($U_{liq-gas}$).

3.3. Technological advancement and optimization

The storage system assessment described above is used to identify the most promising solution, which is then applied to conduct a detailed evaluation of the enhancements in PEMFC technology and their consequent impact on the overall system, following the same procedure illustrated in Fig. 3.

During this stage, a comprehensive evaluation of fuel cell technologies was conducted. This included not only the baseline low-temperature PEMFC commercial model but also data from the literature on three advanced PEMFCs: one low-temperature PEMFC and two high-temperature PEMFCs.

For all fuel cell stacks, process equipment was sized to meet nominal day and night anchoring power requirements, ensuring full operational coverage. The parasitic loads of the BoP were assessed, and the net power outputs were compared to the power demands of the daytime anchorage.

The thermal management system was analysed using both air and seawater as potential heat sinks.

The results provided detailed evaluations of weight, volume, and efficiency for each case, which were then compared to commercial battery systems. Furthermore, power-to-power efficiencies were calculated, enabling an overarching comparison of the various technologies, not only based on gravimetric and volumetric metrics but also in terms of overall system performance.

3.3.1. Fuel cell types

Four types of PEMFC were evaluated: two operating at low temperature and two at high temperature. Each technology included a commercial baseline (LT-PEMFC and HT-PEMFC) and an experimental variant representing potential technological advancements (referred to as LT-PEMFC reinforced and HT-PEMFC reinforced).

For the LT-PEMFC, the previously discussed baseline solution from PowerCell was considered. As a potential advancement in LT-PEMFC technology, the solution proposed by Nikola was referenced [41]. Compared to traditional LT-PEMFCs, this fuel cell can operate at temperatures up to 95°C, offering significant advantages in thermal management. Enhanced membrane electrode assembly (MEA) performance is achieved through optimized membrane architectures that incorporate thermally stable ionomers to prevent radical scavenging. Although still in development, this project has shown promising initial results.

For the commercial case of HT-PEMFC, the Celtec® MEA developed by BASF in collaboration with Advent Technologies and Metal Solutions was referenced [42]. A potential advancement for HT-PEMFC involves using protonated electrodes with phosphonic acid, which promise significant improvements in power density and durability for heavy-duty vehicle applications [43].

The characteristics of the three advanced PEMFCs are reported in Table 2 and compared to the baseline LT-PEMFC from PowerCell, while their corresponding polarization curves are summarized in Fig. 4.

The operating point of the different PEMFCs was determined by applying a heat rejection constraint, a criterion widely adopted in automotive fuel cell applications to ensure the feasibility of the cooling system [44]. In the present study, this criterion is used as an engineering parameter to identify thermally feasible operating points and enable a consistent comparison among different PEMFC technologies, rather than as a strict thermal design constraint.

In this approach, the thermal power generated by the stack (Q, in kW) must be rejected through the available temperature difference ΔT between the stack coolant and the thermal sink (i.e., the ambient environment). The $\frac{Q}{\Delta T}$ ratio therefore represents the thermal load that must be managed per degree of driving temperature difference, which must remain within practical limits to avoid an oversized or impractical cooling system. Operating at higher currents increases Q due to lower efficiency, and without a constraint, this would require excessive cooling capacity, particularly critical in mobile applications such as yachts, where space is limited.

Although the adopted threshold originates from automotive fuel cell

Table 2
Characteristics of the different PEMFC used for the analysis.

	LT-PEMFC	LT-PEMFC reinforced	HT-PEMFC	HT-PEMFC reinforced	Unit
Temperature	80	95	180	160	°C
Pressure	2.5	2.50	1.50	1.50	bar
Rated power density @ 0.6 V	N/A	0.965	0.249	0.443	W cm^{-2}
Cell area	N/A	25	45	45	cm^2
Gravimetric index	N/A	2.51	3.50	3.50	kW kg^{-1}

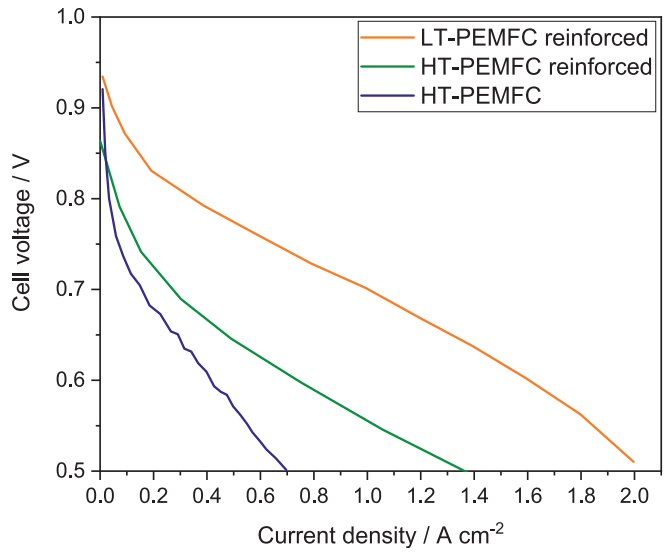

Fig. 4. Polarization curves of the different PEMFC used in the analysis [41–43].

studies, its application in the present work is considered conservative for the investigated yacht case. While seawater cooling offers higher heat rejection potential compared to air-based systems, compact onboard integration remains a key design constraint, making the use of this criterion appropriate for defining realistic operating conditions.

The heat rejection constraint is expressed as [46]:

$$\frac{Q}{\Delta T} = \frac{P_{stack} \cdot \frac{V_t - V}{V}}{T_{stack} - T_{ambient}} < 1.45\ kW^{\circ} C^{-1} \tag{16}$$

where:

- P_{stack}(kW) is the stack rated power,
- V_t(V) is the thermodynamic theoretical cell voltage,
- V(V) is the operating cell voltage,
- ΔT represents the difference between the stack operating temperature T_{stack} (°C) and the temperature of the external environment $T_{ambient}$ (°C).

By fixing this Q/ΔT ratio below a threshold value, the operating voltage and efficiency of each PEMFC configuration are selected accordingly. This ensures that the compared systems are evaluated under thermally feasible and consistent operating conditions, since both efficiency and net power output inherently depend not only on the stack's intrinsic performance but also on auxiliary power requirements related to heat rejection.

Once the operating potential satisfying the aforementioned criterion was selected, the operating current density was derived from the polarization curve. These specifications pertain to a single cell. Next, it was necessary to evaluate the number of cells required to meet the energy demands, starting from the single cell area.

Regarding the stack weight, an evaluation for the LT-PEMFC reinforced was made based on the gravimetric index of 2.51 kW kg^{-1} [24]. For the HT-PEMFC, the gravimetric index of 2 kW kg^{-1} was derived from [45]. However, this gravimetric index refers to the entire fuel cell system, including the weights of components other than the stack itself. To address this issue, HYpoint White Paper was consulted [46], which specifies the weight distribution for a typical HT-PEMFC system, indicating that the fuel cell stack accounts for about 56% of the overall system weight.

The characteristics of the different PEMFCs are reported in Table 2.

4. Results and discussion

This section presents the main outcomes of this work. First, the PEMFC system was designed and its potential contribution to decarbonizing energy demand was assessed. The initial assessment compared the weight, volume and power-to-power efficiency of various storage solutions with those of conventional diesel. Subsequently, detailed analyses of the systems, incorporating technological advancements and optimization strategies, are presented, with an emphasis on weight, volume, and overall system efficiency. Finally, the most promising solution is benchmarked against the marine diesel reference case.

4.1. System design: Analysis of storage solutions for a commercial fuel cell system

Based on the load analysis, the stack should guarantee a net electrical power output capable of covering at least 2/3 of the power demand during day anchor. To be conservative, the PowerCell with maximum stack capacity of 92 kW was selected but, in operation, the stack is limited to 80% of its nominal capacity. This approach accounts for auxiliary system consumption while enabling operation at partial loads, where fuel cell efficiency is inherently higher. Unlike thermal engines, the fuel cell exhibits a decrease in efficiency as its operating power increases. As a result, the oversizing enables to work at higher efficiencies, with relative savings in terms of hydrogen to feed and waste heat to remove. By comparing the sizes of the fuel cell stack and of the entire system from the manufacturer catalogues, it results that the stack represents about 16% of the overall FC system weight and about 11% of its total volume.

As previously discussed, the complete electrical system for hoteling purposes comprises a diesel generator, an electric engine, a PEMFC system, and a battery storage system, as illustrated in Fig. 5(a). While the diesel generator and electric engine are sized to meet the peak power demands during manoeuvring and day cruising (Fig. 5(c)), the integration of the PEMFC system plays a pivotal role in de-fossilizing the vessel's energy supply. Specifically, with the selected energy supply configuration, the PEMFC system enables the de-fossilization of over 80% of the hotelling energy demand. As illustrated in Fig. 5(b), the anchor operation (both day and night) accounts for the majority of the vessel's energy consumption, which is predominantly covered by the PEMFC system.

After defining the power requirement from the fuel cell, the initial phase of the analysis was dedicated to assessing the space and volume requirements for the various fuels, including compressed hydrogen, methanol, and ammonia. The assessment was performed in comparison to marine gas oil (MGO) and results are shown in Table 8. This evaluation specifically focused on yacht sizes ranging from 35 to 45 m in length, as it was deemed impractical for yachts with a length less than 24 m. The results reveal significant challenges, particularly in the context of hydrogen storage solutions, where there is a pronounced need for substantial storage volumes in the case of compressed hydrogen (attributed to its low energy density).

4.1.1. Compressed hydrogen system

First, the sizing of the single tank containing 5 kg of compressed hydrogen was conducted for both 350 bar and 700 bar storage. The results are reported in Table 3.

The reported values were compared with the DOE targets [16], focusing on the weight contribution of each component. Since the other system components align with the DOE targets, the BoP is considered to follow the same percentage distribution as specified by the DOE [16], and thus is expected to be in agreement as well. The results are shown in Table 4.

Finally, the entire system characteristics are reported in Table 5.

4.1.2. Methanol system

In this section the sizing results of the overall methanol system are

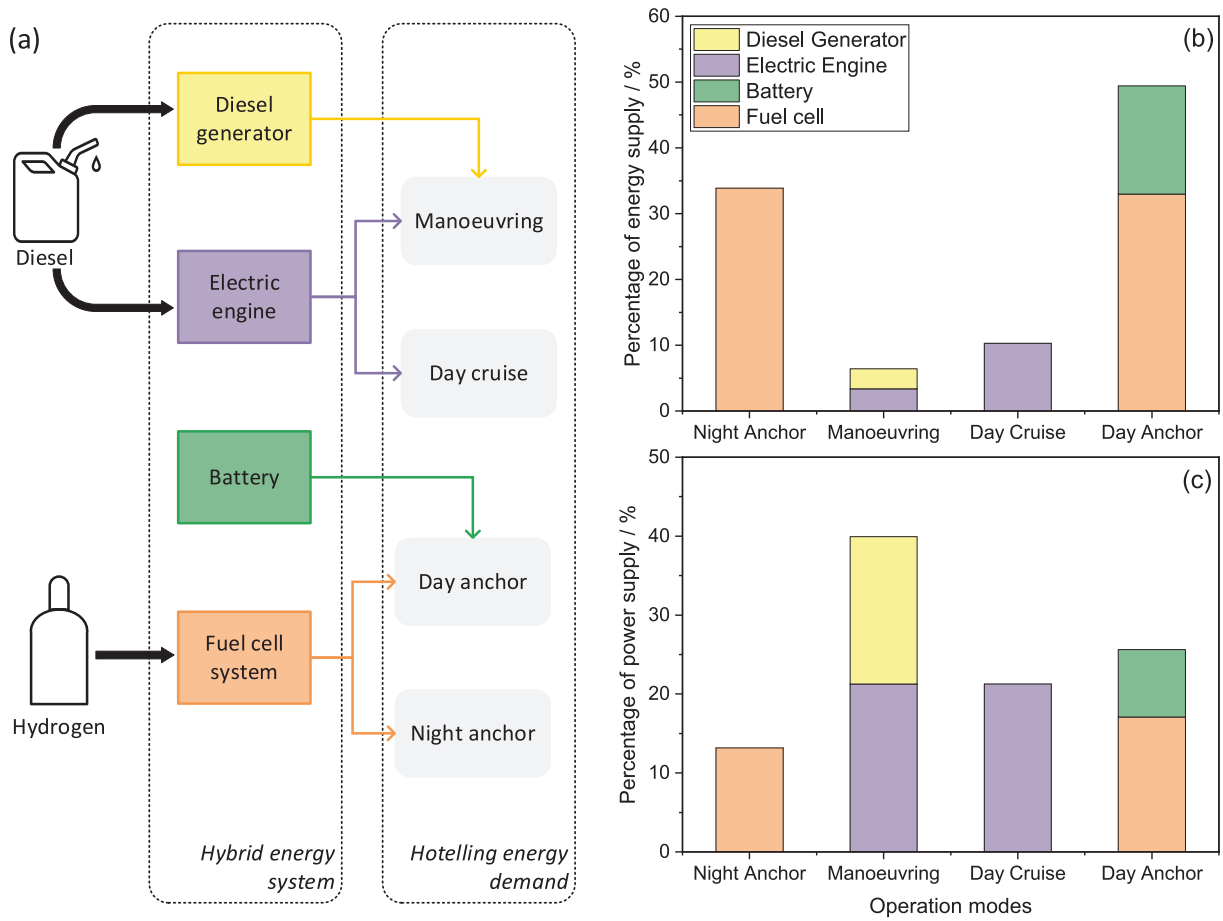

Fig. 5. (a) Simplified scheme of energy allocation among the components of the hybrid system across different operational modes for hoteling requirements; (b) energy distribution percentage and (c) power supply percentage for the same modes in a 35–45 m yacht.

Table 3
Parameters of the single in-pressure tank for storage at 350 bar and 700 bar.

Pressure	350 bar	700 bar
Composite thickness	15 mm	28 mm
Ext. Volume	0.32 m^3	0.22 m^3
Gravimetric index	5.26%wt	4.69%wt
Tank gravimetric energy density	1.63 kWh kg^{-1}	1.46 kWh kg^{-1}
Tank volumetric energy density	620 kWh m^{-3}	890 kWh m^{-3}

Table 4
Comparison of the weight contribution of the different tank layers between data calculated and DOE [16].

Pressure [bar]	350		700	
Category	Calculated	DOE	Calculated	DOE
Compressed H_2	5%	6%	5%	5%
Liner layer	10%	11%	6%	7%
Composite layer	57%	53%	66%	62%
Glass fiber layer	6%	6%	4%	4%
Dome protection	5%	5%	4%	4%
BoP	17%	19%	15%	17%

reported. The amount of methanol derived for the reforming process is based on the day anchor requirement, which is the worse condition, thus it is assumed as reference for the sizing procedure. As shown in Table 6, an additional 25 wt% of methanol is needed to guarantee the thermal requirements of the system (pre-heating of the reactants and temperature control in the reformer) through a combustion process in a dedicated burner. Furthermore, to let the reforming reaction take place, a

Table 5
Weight and volume of the compressed hydrogen storage system for 35–45 m yacht.

Pressure	350 bar	700 bar
Number of tanks real	53	53
System mass	6051 kg	6785 kg
System volume	17.1 m^3	11.9 m^3
UF	0.5	0.5
External volume	34.2 m^3	23.8 m^3

Table 6
Sizing results of methanol-based system with baseline LT-PEMFC.

Component		Mass, kg	Volume, m^3
Storage system	Mass of methanol (reforming + combustion)	2263 + 561	2.38 + 0.59
	Water	992	1.02
	Methanol pump	4.90	0.006
	Water pump	4.90	0.006
Combustion system	Combustor	133	0.78
	Air compressor	307	1.20
Pre-heating of reactants		3.7	0.005
Reforming reactor		525	0.40
Fuel cell	Stack	34.0	0.030
	Air compressor	4.60	0.009
TMS FC with seawater	Heat exchanger	9.50	0.013
	Glysantin	31.0	–
	Auxiliaries	8.10	–
	Water pump	1.10	0.002

tank of water is sized according to Section 3.2.2. While the water requirement has been calculated for completeness, it is not included in the overall weight and volume estimations. This is because the PEMFC generates water that could potentially be recirculated, requiring only a small buffer tank for operational stability. The membrane reactor is oversized to guarantee the maximum hydrogen flow rate of the day anchor. Subsequently, fuel cell system with commercial LT-PEMFC technology and seawater-cooled TMS is evaluated. Seawater is selected as the most significative option both in terms of weight and volume reduction of the heat exchanger, since the liquid–liquid heat transfer is higher than the gas–liquid. Particularly, a 63% weight reduction of the TMS is observed compared to air cooling.

To better comprehend the results and visualize the impact of each component on the overall system, the distribution of weight (Fig. 6(a)) and volume (Fig. 6(b)) are reported. The storage system emerged as the primary contributor in both weight and volume, even excluding the amount required for water storage, as this can be easily accommodated onboard the yacht. While the auxiliaries, which include all the equipment of the BoP (i.e. pumps, compressors, heat exchangers and combustor), have a major impact mainly on the volume of the system. Furthermore, the fuel cell system, including FC stack and seawater cooling, has the lowest effect compared to other components.

In addition, opting for a see-water cooled TMS offers advantages from an electrical power perspective. As shown in Fig. 7, for the same electrical power output of 72.9 kW, the net power with seawater cooling (59.1 kW) is higher than with air cooling (50.4 kW) due to lower electrical losses. This improvement primarily stems from the lower energy required to pump seawater through a heat exchanger (Fig. 7(b)), compared to the electrical demand of a fan (Fig. 7(a)). In both cases, the oversizing of the fuel cell stack ensures the hoteling demands are fully met, both during day and night anchorage.

4.1.3. Ammonia system

This section states the sizing results of the ammonia system. As shown in Table 7, a 34 wt% of ammonia is required to guarantee the thermal demands of the system through a combustion process. The reactor of ammonia cracking is quite light and compact. Subsequently, fuel cell system with commercial LT-PEMFC technology and seawater cooling is assessed.

As already discussed in the previous paragraph, to graphically display the weight of each component on the overall system, the distribution of weight (Fig. 8 (a)) and volume (Fig. 8 (b)) are reported.

As in the case of methanol, the storage system is the main contributor both in terms of weight and volume, followed by the auxiliaries which have a greater impact on the system volume. Conversely, the FC system, including the stack and the seawater cooling system, and the reactor have an almost negligible impact.

Also with this storage solution, the adoption of a seawater-cooled TMS further enhances the net electrical power output. According to Fig. 9, the electrical consumption of the auxiliary equipment is significantly higher with the air-cooled system (Fig. 9(a)). It is important to note that the seawater-cooled configuration (Fig. 9(b)) provides greater usable net power, allowing for the possibility of reducing the level of oversizing required for the system. By using seawater instead of air, the TMS weight was reduced by 63%.

4.1.4. Storage solutions comparison

In this section, the weight, volume, and efficiency of the different storage methods are compared to determine the most suitable solution.

First, the weight and volume are compared relative to the current marine gas oil (MGO), which is assigned a reference value of 1 for both volume and weight. The results are summarized in Table 8.

Compressed hydrogen at 350 bar requires significantly larger storage volumes—approximately 25 times that of MGO —and leads to a weight increase of 4.2 times compared to MGO. Increasing the pressure from 350 bar to 700 bar reduces the storage volume by about 30% due to the higher density of hydrogen. However, even with this reduction, the required volume remains considerably larger than the available space on a luxury vessel. Furthermore, the higher pressure results in an increased weight, as the storage tank must be designed to withstand these elevated pressures, necessitating thicker walls.

Methanol and ammonia, as alternative options, exhibit more manageable increase in required weight and volume compared to compressed hydrogen. Specifically, ammonia is advantageous if weight is the primary constraint, while methanol is more suitable when volume is the main concern.

These estimates are accurate for compressed hydrogen due to its simpler storage system but may be optimistic for chemical storage. Methanol and ammonia storage require additional components besides the fuel tank, leading to further increases in system weight and volume. However, the results remain fairly representative as the key components that significantly impact system weight and volume (i.e., reactor, fuel tank and main auxiliaries) were considered.

Finally, the different storage solutions are compared in terms of efficiency. First, the chemical-to-power efficiency (η_{CTP}), defined as the capacity to convert fuel into usable electrical energy, was calculated as follows:

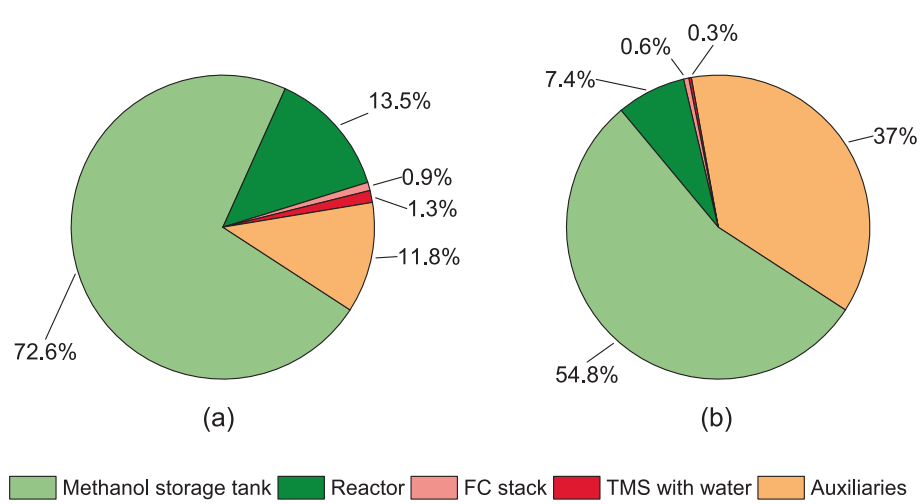

Fig. 6. Methanol-based system: Distribution of weight (a) and volume (b) of methanol-based system with baseline LT-PEMFC and seawater-cooled, liquid-based TMS.

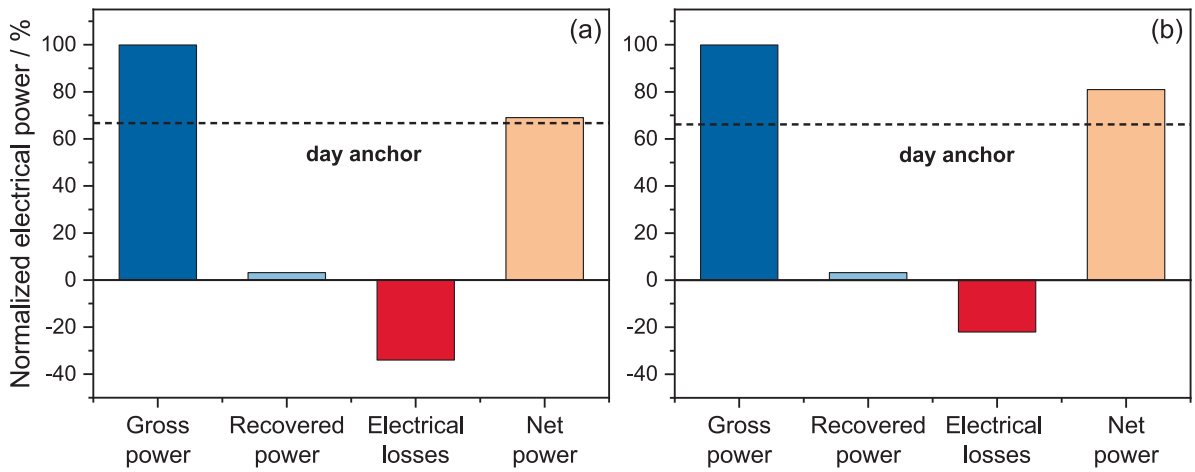

Fig. 7. Electric power distribution for methanol-based system, normalized to the PEMFC gross power output, in the case of (a) air-cooled liquid-based TMS and (b) seawater-cooled liquid-based TMS.

Table 7
Sizing results of ammonia-based system with baseline LT-PEMFC.

Component		Mass, kg	Volume, m^3
Storage system	Mass of ammonia (cracking + combustion)	1770 + 631	4.00 + 1.40
	Tank	84.5	5.40
Combustion system	Combustor	120	0.79
	Air compressor	196	0.77
Pre-heating of reactants		4.50	0.010
Cracking reactor		8.70	0.011
Fuel cell	Stack	34.0	0.030
	Air compressor	4.60	0.009
TMS FC with seawater	Heat exchanger	9.50	0.013
	Glysantin®	31.0	–
	Auxiliaries	8.10	–
	Water pump	1.10	0.002

Table 8
Comparative factors for weight and volume of different storage solutions compared to MGO.

	MGO	Compressed hydrogen 350 bar	Compressed hydrogen 700 bar	Methanol	Ammonia
Weight	x 1	x 4.2	x 4.7	x 3.9	x 2.9
Volume	x 1	x 25.1	x 17.5	x 6.0	x 7.8

$$\eta_{CTP} = \frac{P_{net}}{\dot{m}_{carrier} \cdot LHV_{carrier}} \tag{17}$$

where P_{net} (kW) is the net power output under day anchor condition which is the most demanding in terms of energy consumption, $\dot{m}_{carrier}$ (kg s^{-1}) is the total flow rate of the energy carrier and $LHV_{carrier}$ (MJ kg^{-1}) represents its lower heating value.

Subsequently, the power-to-power efficiency (η_{PTP}) was estimated according to the relationship:

$$\eta_{PTP} = \eta_{CTP} \cdot \eta_{WTT} \tag{18}$$

Here, η_{WTT} represents the well-to-tank efficiency, which reflects the efficiency involved in the production of the energy carrier.

From the comparison of the efficiencies of the three storage methods in Table 9, it is evident that compressed hydrogen offers the best power-to-power efficiency. This is because hydrogen is stored in its pure form, avoiding the efficiency losses associated with conversion and reconversion processes. Moreover, ammonia emerges as more efficient than methanol, thanks to its superior thermal integration capability.

4.2. Technological advancement and optimization

Based on the findings from the storage system sizing analysis, methanol emerged as the most suitable option for onboard use due to the primary requirement of minimizing volume. Additionally, methanol is considered safer than ammonia as a fuel for marine applications. Unlike ammonia, which is highly toxic, corrosive, and requires advanced safety measures to manage risks such as accidental leaks, methanol is less hazardous to handle and store. Its liquid state at ambient conditions simplifies onboard storage and integration compared to ammonia, which requires pressurization or cryogenic systems. These factors make methanol a more practical and safer choice for use on small yachts, where no specialized crew is available for the handling of dangerous fuels. Therefore, as explained in Section 3.1, several optimization strategies for PEMFC technology have been investigated focusing on methanol as energy carrier.

First, the operational point of the fuel cell technology was defined for the various case studies with the aim of minimizing the $Q/\Delta T$ ratio, as outlined in Section 3.3.1. This approach ensures optimal thermal management and efficient system performance. In all case studies, the fuel cell stack was designed to deliver a nominal power output of 92 kW, consistent with the baseline PowerCell case. To achieve this, the number of cells in the stack was determined based on the output of each individual cell, ensuring the total output met the nominal conditions of the baseline PowerCell.

Table 10 presents the results for the different PEMFC case studies, detailing key parameters such as the actual operational voltage and the stack efficiency under sizing conditions, the effective $Q/\Delta T$ ratio, and the operating pressure and temperatures. These results highlight the influence of different configurations and optimization strategies on system performance.

After defining the operating points of the different PEMFC technologies, the focus shifted to estimating the weight of the TMS, which is typically a significant factor in such application. This analysis allows for a meaningful comparison between the various fuel cell technologies.

From Fig. 10(a), it is evident that optimizing the fuel cell system can substantially reduce the impact of the TMS. For instance, the LT-PEMFC reinforced configuration achieves a significant 46.2% reduction in TMS weight compared to the baseline LT-PEMFC. This improvement is due to higher efficiency (60.4% compared to 56.5%), which reduces the heat generated, as well as an increase in operating temperature from 80°C to 95°C.

Increasing the operating temperature with HT-PEMFC configurations, despite their lower efficiency, also leads to a reduction in TMS, approaching 40%.

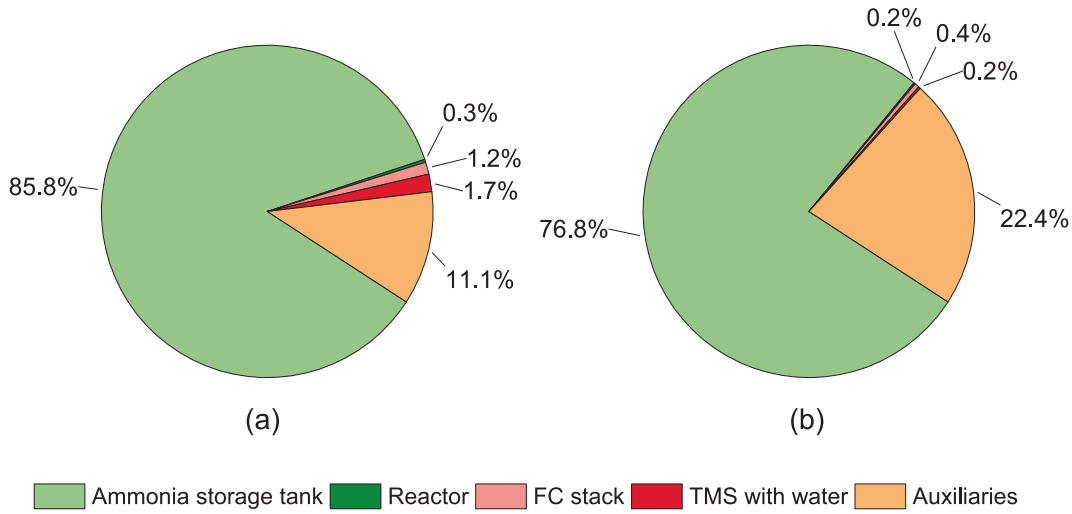

Fig. 8. Ammonia-based system: Distribution of weight (a) and volume (b) of ammonia-based system with baseline LT-PEMFC and seawater-cooled, liquid-based TMS.

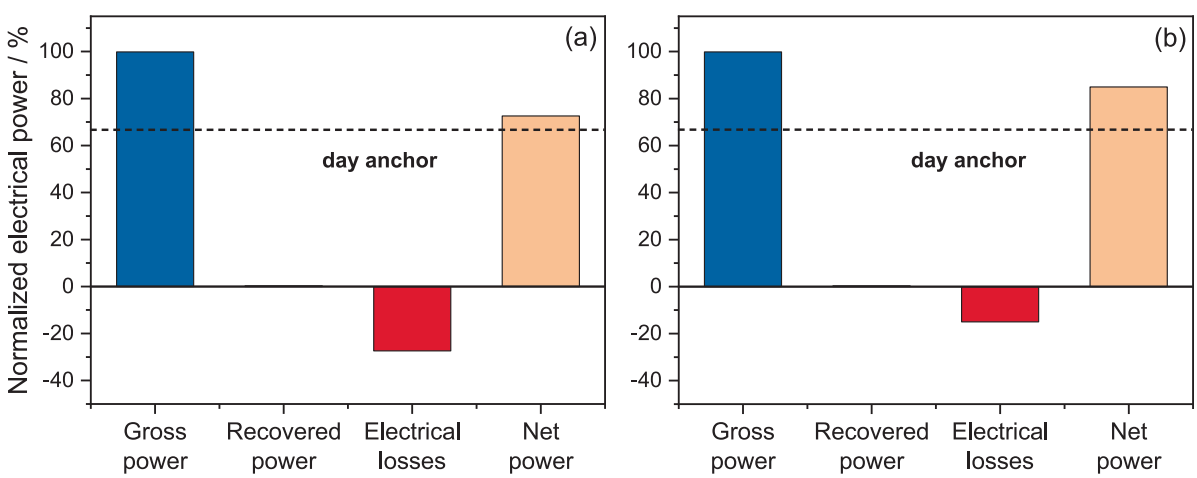

Fig. 9. Electric power distribution for ammonia-based system, normalized to the PEMFC gross power output, in the case of (a) air-cooled liquid-based TMS and (b) seawater-cooled liquid-based TMS.

Table 9
Comparison of efficiencies for the different energy carriers.

	η_{WTT} [15]	η_{CTP}	η_{PTP}
Compressed hydrogen	60.0%	49.4%	29.6%
Methanol	41.0%	41.7%	17.1%
Ammonia	54.0%	43.2%	23.3%

Furthermore, switching from an air-cooled liquid-based TMS to a seawater-cooled liquid-based TMS results in additional weight savings, as reported in Fig. 10(b). This outcome is not surprising, as liquid-to-liquid heat exchange is significantly more efficient than gas-to-liquid heat transfer, owing to much higher heat transfer coefficients. Notably, the quantity of Glysantin® used remains unchanged, as the total heat to be dissipated does not vary regardless of whether air or seawater is utilized in the open-loop system. The main differences between the two cooling approaches lie in the weight of the heat exchanger and, consequently, the auxiliaries. These changes account for the percentage weight reductions highlighted in Fig. 10(b).

The various PEMFC configurations were subsequently integrated with a methanol storage system. Table 11 summarizes the main outcomes regarding the weight, volume, and efficiencies for the complete methanol-based system coupled with enhanced PEMFC solutions.

The results of this analysis demonstrate that, although HT-PEMFC technology potentially offers better thermal management due to its higher operating temperature, it is characterized by lower efficiencies. These lower efficiencies limit the technology's performance, requiring larger amounts of fuel and negating the advantages in the TMS.

Table 10
Operative conditions of different PEMFC case studies.

	Stack power output	Operating voltage @ sizing point	Stack efficiency @ sizing point	Q/dT	Pressure	Temperature	Net power output
Baseline: LT-PEMFC	92 kW	0.68 V	56.5%	–	2.5 bar	80°C	59.1 kW
LT-PEMFC reinforced	92 kW	0.76 V	60.4%	1.08	2.5 bar	95°C	60.2 kW
HT-PEMFC	92 kW	0.57 V	45.3%	0.78	1.5 bar	180°C	60.7 kW
HT-PEMFC reinforced	92 kW	0.65 V	51.2%	0.72	1.5 bar	160°C	61.9 kW

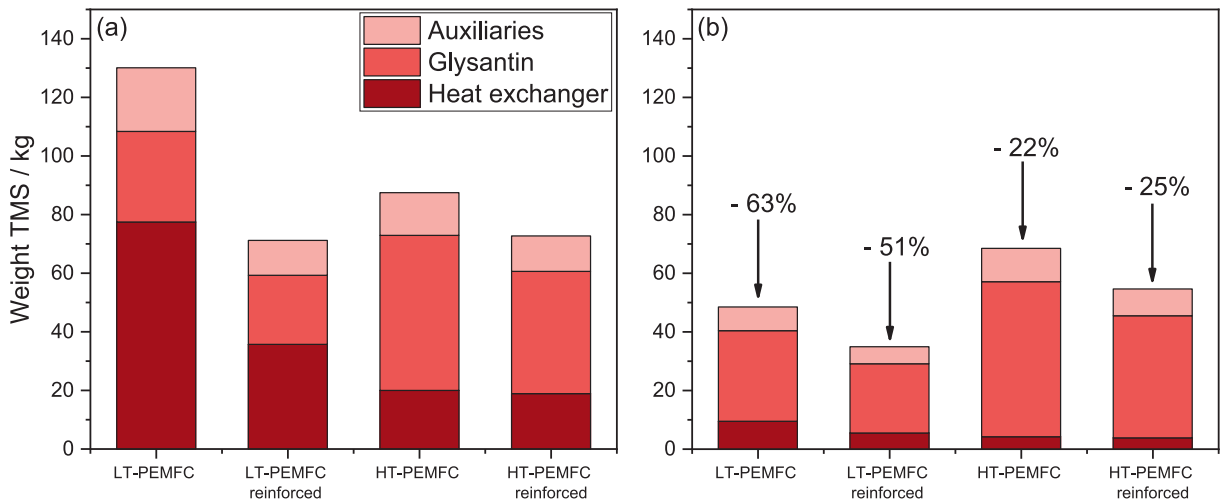

Fig. 10. Comparison of TMS component weights for methanol-based system with different PEMFC technologies, in the case of (a) air-cooled liquid-based TMS and (b) seawater-cooled liquid-based TMS.

Table 11
Comparison of different PEMFC technologies in the methanol-based system with seawater-cooled TMS.

	LT-PEMFC baseline	LT-PEMFC reinforced	HT-PEMFC	HT-PEMFC reinforced	
Storage system mass	4882	4558	6090	5325	kg
Storage system volume	6.44	6.03	7.95	7.06	m^3
Net electrical power output	59.1	60.2	60.7	61.9	kW
η_{CTP}	42	46	35	40	%
η_{PTP}	17	19	14	16	%

Conversely, an optimized low-temperature PEMFC solution can provide significant benefits to the system. Specifically, it slightly increases the chemical-to-power efficiency from 41.7% in the baseline configuration to 46% in the optimized LT-PEMFC reinforced case, representing an efficiency improvement of approximately 10.3%. This leads to a reduction in storage weight by approximately 6.7% and a reduction in storage volume by approximately 6.4%.

5. Conclusions

This paper investigates the feasibility of hydrogen-powered fuel cell electrification to meet the hoteling demands onboard a 35–45 m yacht, with a focus on various onboard hydrogen storage methods. Specifically, the study examines physical storage, using compressed hydrogen at 350 bar and 700 bar, as well as chemical storage in the form of methanol and ammonia. The storage systems were carefully sized to address the unique requirements of onboard applications, including the integration of conversion units for producing pure hydrogen where necessary. A detailed analysis was conducted to evaluate the storage solutions and conversion systems, considering their impacts on weight, volume, and overall efficiency.

The findings underscore that, within the investigated yacht case study, green methanol and green ammonia represent the most viable solutions for onboard application. Ammonia offers competitive advantages in terms of weight savings and higher chemical-to-power efficiency, but it is constrained by lower safety standards and increased volume demand. On the other hand, methanol emerged as the most suitable option for onboard use due to the primary requirement of minimizing space onboard the yacht.

The implementation of a seawater-cooled, liquid-based thermal management system further enhances the feasibility of these solutions by reducing system weight and improving thermal management efficiency, especially when operating at higher temperatures.

By integrating advanced PEMFC technologies, including both low-temperature and high-temperature configurations, and their potential enhancements, the study demonstrates the critical role of fuel cell optimization in achieving substantial performance improvements. For instance, the adoption of reinforced LT-PEMFC solutions improves chemical-to-power efficiency, reduces heat generation, and allows for lighter and more compact thermal management systems.

Overall, this work highlights the importance of adopting a holistic approach to de-fossilization in the yachting sector. Combining efficient power devices with strategic use of chemical carriers provides a pathway to sustainable onboard energy systems for this specific maritime segment. The results not only emphasize the need to optimize power-to-power efficiency but also reveal the trade-offs between safety, energy density, and system integration in selecting the most suitable energy carrier storage method.

Although the quantitative outcomes of the present study are specific to the investigated yacht application and should not be directly extrapolated to fundamentally different vessel categories, the integrated assessment methodology and system-level design approach developed in this work may provide a valuable reference framework for evaluating alternative fuel cell-based energy solutions in other maritime applications.

Future research should focus on addressing remaining challenges, such as improving the safety profile of ammonia and exploring additional advancements in fuel cell technology, to further enhance the sustainability and practicality of zero-emission yachts and to assess the applicability of these findings to other maritime contexts.

CRediT authorship contribution statement

Maria Chiara Massaro: Writing – review & editing, Writing – original draft, Visualization, Methodology, Investigation, Formal analysis, Data curation, Conceptualization. **Elisa Revello:** Writing – review & editing, Writing – original draft, Visualization, Software, Methodology, Investigation, Formal analysis, Data curation. **Paolo Marocco:** Writing – review & editing, Validation, Supervision, Investigation. **Massimo Santarelli:** Writing – review & editing, Supervision, Resources. **Marta Gandiglio:** Writing – review & editing, Visualization, Supervision, Project administration, Investigation, Funding acquisition, Conceptualization. **Alessandro Monteverde:** Writing – review &

editing, Supervision, Resources, Project administration, Investigation, Conceptualization.

Declaration of competing interest

The authors declare that they have no known competing financial interests or personal relationships that could have appeared to influence the work reported in this paper.

Acknowledgements

The authors would like to express their gratitude to Azimut|Benetti Group for their support and valuable contributions to the development of this study. The authors would also like to acknowledge the support provided by Leonardo S.p.A. through the funding of M.C. Massaro and E. Revello's doctoral scholarships. Special thanks to Elena Rosa Loizzo and Lorenzo D'Agnano for their contribution to data analysis during their master's theses, which provided a foundation for this study. The project is supported by the Clean Hydrogen Partnership and its members under Grant Agreement No 101137586 (IMAGHYNE project).

Appendix A. Input data

Table A summarizes all key modelling inputs adopted in this study, together with their source classification, in order to ensure transparency and traceability of the modelling assumptions. Parameters classified as engineering estimates represent the main sources of uncertainty in the model. Where applicable, conservative assumptions have been adopted (e.g., worst-case cooling conditions and upper-bound conversion performance) to ensure robustness of the results.

Table A
Comprehensive input data for the sizing model.

Subsystem	Input parameter	Value	Unit	Source
Compressed hydrogen system	Mass of hydrogen per tank, $m_{H_2,tank}$	5	kg	[28]
	Liner thickness, t_{liner}	5	mm	Engineering estimation (consistent with DOE-based system design [28])
	Liner density, ρ_{liner}	960	kg m^{-3}	Physical property
	Composite density, $\rho_{composite}$	1580	kg m^{-3}	Physical property
	Stress equilibrium factor, k_s	0.75	–	[29]
	Burst pressure, p_b	90	MPa	[28]
	Glass fiber thickness, t_{glass}	1	mm	Engineering estimation (consistent with DOE-based system design [28])
	Glass fiber density, ρ_{glass}	2480	kg m^{-3}	Physical property
	Foam thickness, t_{foam}	10	mm	Engineering estimation (consistent with DOE-based system design [28])
	Foam density, ρ_{foam}	675	kg m^{-3}	Physical property
	BoP mass, m_{BoP}		kg	[28]
Methanol storage system	Gravimetric index methanol tank	4.03	kWh kg^{-1}	[15]
	Volumetric index methanol tank	3.83	kWh L^{-1}	[15]
	Methanol conversion	>90	%	[47]
	Hydrogen purity	>99.9	%	Engineering estimation
	Hydrogen recovery	>90	%	Engineering estimation
Ammonia storage system	Yield strength ammonia tank, $R_{p,0.2}$ (at 20°C)	200	MPa	Physical property (AISI 316)
	Tensile strength ammonia tank, R_m (at 20°C)	515	MPa	Physical property (AISI 316)
	Density ammonia tank, ρ (at 20°C)	806	kg m^{-3}	Physical property (AISI 316)
	Safety empty volume of the tank	14	% of total volume	Engineering estimation
	Ammonia conversion	100	%	[48]
	Hydrogen purity	>99.97	%	[48]
	Hydrogen recovery	>90	%	[48]
	Gravimetric index cracking reactor	8123	kg kg^{-1}	Engineering estimation from equivalent intensified reactor in [35]
	Volumetric index cracking reactor	9.9	m^3 kg^{-1} s	Engineering estimation from equivalent intensified reactor in [35]
Cooling system	Coolant temperature difference, ΔT	10	°C	Engineering estimation
	Coolant specific heat capacity, $c_{p,coolant}$	3.00–3.55	kJ kg^{-1} K^{-1}	[38]
	Coolant circulation time, $t_{circ,coolant}$	20	s	[40]
	Inlet air temperature in the radiator, $T_{in,air}$	40	°C	Engineering estimation
	Outlet air temperature from the radiator, $T_{out,air}$	55	°C	Engineering estimation
	Air specific heat capacity, $c_{p,air}$	1.0035	kJ kg^{-1} K^{-1}	Engineering estimation
	Overall liquid–gas heat transfer coefficient, $U_{liq-gas}$	70	W m^{-2} K^{-1}	[45]
	Inlet seawater temperature in the heat exchanger, $T_{in,seawater}$	23	°C	Engineering estimation
	Outlet seawater temperature from the heat exchanger, $T_{out,seawater}$	38	°C	Engineering estimation
	Seawater specific heat capacity, $c_{p,seawater}$	4.00	kJ kg^{-1} K^{-1}	Physical property
	Overall liquid–liquid heat transfer coefficient, $U_{liq-liq}$	284	W m^{-2} K^{-1}	[49]
	TMS gravimetric index, w	1.08	kg m^{-2}	[45]
	TMS volumetric index, v	700	m^2 m^{-3}	[45]
	Fouling resistance for seawater (<325 K)	0.00009	m^2 K W^{-1}	[50]

(continued on next page)

Table A (*continued*)

Subsystem	Input parameter	Value	Unit	Source
	TMS BoP	20	% of TMS weight	Engineering estimation
Fuel cell	LT-PEMFC reinforced stack gravimetric index	2.51	kW kg^{-1}	Engineering estimation from [24]
	HT-PEMFC stack gravimetric index	0.56x2	kW kg^{-1}	Engineering estimation from [45 46]

Data availability

The data that has been used is confidential.

References

[1] International Maritime Organization (IMO), 2023 IMO Strategy on Reduction of GHG Emissions from Ships; 2023. https://www.imo.org/en/OurWork/Environment/Pages/2023-IMO-Strategy-on-Reduction-of-GHG-Emissions-from-Ships.aspx (accessed April 2, 2024).

[2] International Maritime Organization (IMO), Improving the energy efficiency of ships; 2024. https://www.imo.org/en/OurWork/Environment/Pages/Improving%20the%20energy%20efficiency%20of%20ships.aspx (accessed April 5, 2024).

[3] Wang Y, Maidment H, Boccolini V, Wright L. Life cycle assessment of alternative marine fuels for super yacht. Reg Stud Mar Sci 2022;55. https://doi.org/10.1016/j.rsma.2022.102525.

[4] Wang X, Zhu J, Han M. Industrial Development Status and prospects of the Marine fuel Cell: a Review. J Mar Sci Eng 2023;11. https://doi.org/10.3390/jmse11020238.

[5] K. Damborsky, Sanlorenzo to deliver first 50Steel in 2024, (2023). https://www.boatinternational.com/yachts/news/first-sanlorenzo-50steel (accessed April 9, 2024).

[6] Engelhardt P, Maximini M, Beckmann F, Brenner M. Integrated fuel cell APU based on a compact steam reformer for diesel and a PEMFC. Int J Hydrogen Energy 2012;37:13470–7. https://doi.org/10.1016/j.ijhydene.2012.06.080.

[7] Malla U. Design and sizing of battery system for electric yacht and ferry. Int J Interact Des Manuf 2020;14:137–42. https://doi.org/10.1007/s12008-019-00622-2.

[8] Bucci V, Mauro F, Vicenzutti A, Bosich D, Sulligoi G. Hybrid-electric solutions for the propulsion of a luxury sailing yacht. In: Proceedings - 2020 2nd IEEE International Conference on Industrial Electronics for Sustainable Energy Systems, IESES 2020; 2020. p. 280–286. https://doi.org/10.1109/IESES45645.2020.9210696.

[9] T. Coppola, L. Micoli, R. Russo, Concept design and feasibility study of propulsion system for yacht: innovative hybrid propulsion system fueled by methanol, in: 2022 International Symposium on Power Electronics, Electrical Drives, Automation and Motion, SPEEDAM 2022, 2022: pp. 683–688. https://doi.org/10.1109/SPEEDAM53979.2022.9841984.

[10] Micoli L, Russo R, Coppola T. Advancing zero-emission maritime solutions: Case study of an ammonia-powered fuel cell system implementation. Energy Convers Manage: X 2024;22. https://doi.org/10.1016/j.ecmx.2024.100588.

[11] Di Bernardo R, Di Cecca B, Coppola T, Spazzafumo G, Speranza D. Preliminary design of a 75 m mega Yacht with diesel - Electric hybrid propulsion powered with hydrogen FCs. Int J Hydrogen Energy 2024. https://doi.org/10.1016/j.ijhydene.2024.06.412.

[12] Chen M, Savguira Y, MacInnis J, James BD, Thorpe SJ. Power-to-gas: Amphibious yacht and fueling station. Int J Hydrogen Energy 2019;44:31646–69. https://doi.org/10.1016/j.ijhydene.2019.09.158.

[13] Mallouppas G, Yfantis EA. Decarbonization in shipping industry: a review of research, technology development, and innovation proposals. J Mar Sci Eng 2021;9. https://doi.org/10.3390/jmse9040415.

[14] McKinlay CJ, Turnock SR, Hudson DA. Route to zero emission shipping: Hydrogen, ammonia or methanol? Int J Hydrogen Energy 2021;46:28282–97. https://doi.org/10.1016/j.ijhydene.2021.06.066.

[15] Stolz B, Held M, Georges G, Boulouchos K. Techno-economic analysis of renewable fuels for ships carrying bulk cargo in Europe. Nat Energy 2022;7:203–12. https://doi.org/10.1038/s41560-021-00957-9.

[16] Hua TQ, Ahluwalia RK, Peng JK, Kromer M, Lasher S, McKenney K, et al. Technical assessment of compressed hydrogen storage tank systems for automotive applications. Int J Hydrogen Energy 2011;36:3037–49. https://doi.org/10.1016/j.ijhydene.2010.11.090.

[17] Tang D, Tan GL, Li GW, Liang JG, Ahmad SM, Bahadur A, et al. State-of-the-art hydrogen generation techniques and storage methods: a critical review. J Energy Storage 2023;64. https://doi.org/10.1016/j.est.2023.107196.

[18] Rivard E, Trudeau M, Zaghib K. Hydrogen storage for mobility: a review. Materials 2019;12. https://doi.org/10.3390/ma12121973.

[19] J. Anders, Comparison of Alternative Marine Fuels SEA\LNG Ltd, (2019). www.dnvgl.com.

[20] Methanol: A Future-Proof Fuel A Primer Prepared for the Methanol Institute, 2020. https://futurefuelstrategies.com/.

[21] van Biert L, Godjevac M, Visser K, Aravind PV. A review of fuel cell systems for maritime applications. J Power Sources 2016;327:345–64. https://doi.org/10.1016/j.jpowsour.2016.07.007.

[22] DNV, Alternative fuels for containerships; 2023. https://www.dnv.com/maritime/publications/alternative-fuels-for-containerships-methanol-and-ammonia-download/ (accessed April 20, 2023).

[23] Massaro MC, Aluia F, Biga R, Accardo G, Antonio Monteverde AH. Potential of ammonia as hydrogen storage for future electrified aircraft. Energy Convers Manage: X 2025:101034. https://doi.org/10.1016/j.ecmx.2025.101034.

[24] Massaro MC, Biga R, Kolisnichenko A, Marocco P, Monteverde AHA, Santarelli M. Potential and technical challenges of on-board hydrogen storage technologies coupled with fuel cell systems for aircraft electrification. J Power Sources 2023;555. https://doi.org/10.1016/j.jpowsour.2022.232397.

[25] ECHA, European Chemicals Agency registration. dossier; 2025.

[26] Business Wire, Advent Technologies and a Leading Global Energy Technology Company to Develop a Marine Fuel Cell Solution for Superyachts, (2023). https://www.businesswire.com/news/home/20230209005401/en/ (accessed June 27, 2024).

[27] PowerCell Cellution, datasheet; 2023. www.powercellgroup.com (accessed May 4, 2023).

[28] Mcwhorter S, Ordaz G. DOE Fuel Cell Technologies Office Record 13010: Onboard Type IV Compressed Hydrogen Storage Systems - Current Performance and Cost 1301. https://www.hydrogen.energy.gov/docs/hydrogenprogramlibraries/pdfs/review13/st001_ahluwalia_2013_o.pdf.

[29] Zhang Q, Xu H, Jia X, Zu L, Cheng S, Wang H. Design of a 70 MPa type IV hydrogen storage vessel using accurate modeling techniques for dome thickness prediction. Compos Struct 2020;236. https://doi.org/10.1016/j.compstruct.2020.111915.

[30] Plastic Mart, Marine Water Tanks, (2023). https://www.plastic-mart. com/rv-water-waste-holding-tanks/marine-water-tanks/. (accessed January 7, 2024).

[31] Zelenka J, Wermuth N, Lackner M, Wimmer A, Moeyaert P, Marine Benjamin Jäger EN, Lang M, Huschenbett M. Wien GmbH Reddy Devalapalli H. The HyMethShip Project: Innovative Emission Free Propulsion for Ships 5-Low Carbon Combustion-What are the Alternative Fuels for the Future; 2019. https://www.cimac.com.

[32] Jazani O, Bennett J, Liguori S. Carbon-low, renewable hydrogen production from methanol steam reforming in membrane reactors – a review. Chem Eng Process - Process Intesif 2023;189. https://doi.org/10.1016/j.cep.2023.109382.

[33] Perry RH. Perry's chemical engineers' handbook. N Y 1984.

[34] Cerrillo JL, Morlanés N, Kulkarni SR, Realpe N, Ramírez A, Katikaneni SP, et al. High purity, self-sustained, pressurized hydrogen production from ammonia in a catalytic membrane reactor. Chemical Engineering Journal 431 2022. https://doi.org/10.1016/j.cej.2021.134310.

[35] Mazzone S, Campbell A, Zhang G, García-García FR. Ammonia cracking hollow fibre converter for on-board hydrogen production. Int J Hydrogen Energy 2021;46:37697–704. https://doi.org/10.1016/j.ijhydene.2021.09.038.

[36] K.I. Al-Malah, Aspen plus: chemical engineering applications, 2017.

[37] Nguyen HQ, Shabani B. Proton exchange membrane fuel cells heat recovery opportunities for combined heating/cooling and power applications. Energy Convers Manag 2020;204. https://doi.org/10.1016/j.enconman.2019.112328.

[38] BASF, GLYSANTIN® FC G20® ELECTRIFIED Brochure; 2024. https://www.glysantin.com/global/en.html (accessed April 18, 2024).

[39] R.K. Shah, Basic Thermal Design Theory for Recuperators, in: J.& S. Wiley (Ed.), Fundamentals of Heat Exchanger Design (Pp. 97-231), 2007th ed., 2003.

[40] Link A, Ludowicy J, Staggat M. ASSESSMENT OF a SERIAL COOLING CONCEPT FOR HTPEM FUEL CELL SYSTEMS FOR AVIATION APPLICATIONS. 33rd Congress of the International Council of the Aeronautical Sciences. 2022. https://www.icas.org/ICAS_ARCHIVE/ICAS2022/data/papers/ICAS2022_0456_paper.pdf.

[41] Barker A. Advanced Membranes for Heavy Duty fuel. Cell Trucks 2022. https://www.hydrogen.energy.gov/docs/hydrogenprogramlibraries/pdfs/review22/fc333_baker_2022_o-pdf.pdf.

[42] BASF, Celtec ®-P membrane electrode assemblies for high-temperature PEM fuel cells; 2024. https://chemicals.basf.com (accessed June 25, 2024).

[43] Lim KH, Lee AS, Atanasov V, Kerres J, Park EJ, Adhikari S, et al. Protonated phosphonic acid electrodes for high power heavy-duty vehicle fuel cells. Nat Energy 2022;7:248–59. https://doi.org/10.1038/s41560-021-00971-x.

[44] Ahluwalia RK, Wang X, Steinbach AJ. Performance of advanced automotive fuel cell systems with heat rejection constraint. J Power Sources 2016;309:178–91. https://doi.org/10.1016/j.jpowsour.2016.01.060.

[45] Schmelcher M, Häßy MarcSchmelcher J. Hydrogen fuel cells for aviation? a potential analysis comparing different thrust categories. ISABE 2022. https://drive.google.com/drive/folders/16p4Q5zzRB6qFtilPvGWR7cov6IjO2CGO.

[46] HyPoint Inc., White Paper HyPoint, (2021). https://hypoint.com/ (accessed March 23, 2022).

[47] Zelenka J, Wermuth N, Lackner M, Wimmer A, Moeyaert P, Marine Benjamin Jäger EN, Lang M, Huschenbett M, Wien GmbH Reddy Devalapalli H. The HyMethShip

Project: Innovative Emission Free Propulsion for Ships 5-Low Carbon Combustion-What are the Alternative Fuels for the Future; 2019. https://www.cimac.com.
[48] Cerrillo JL, Morlanés N, Kulkarni SR, Realpe N, Ramírez A, Katikaneni SP, Paglieri SN, Lee K, Harale A, Solami B, Jamal A, Mani Sarathy S, Castaño P, Gascon J. High purity, self-sustained, pressurized hydrogen production from ammonia in a catalytic membrane reactor. Chem Eng J 2022;431. https://doi.org/10.1016/j.cej.2021.134310.
[49] D.Q. Kern, Process Heat Transfer, New York, 1950.
[50] Engineering Toolbox, Heat Exchangers - Fouling and Reduced Heat Transfer; 2026. https://www.engineeringtoolbox.com/fouling-heat-transfer-d_1661.html (accessed April 10, 2026).